BOOTSTRAP SAMPLING RATE GREATER THAN 1.0 MAY IMPROVE RANDOM FOREST PERFORMANCE

Anonymous authors
Paper under double-blind review

ABSTRACT

Random forests utilize bootstrap sampling to create an individual training set for each component tree. This involves sampling with replacement, with the number of instances equal to the size of the original training set (N). Research literature indicates that drawing fewer than N observations can also yield satisfactory results. The ratio of the number of observations in each bootstrap sample to the total number of training instances is called the bootstrap rate (BR). Sampling more than N observations (BR > 1) has been explored in the literature only to a limited extent and has generally proven ineffective. In this paper, we re-examine this approach using 36 diverse datasets and consider BR values ranging from 1.2 to 5.0. Contrary to previous findings, we show that such parameterization can result in statistically significant improvements in classification accuracy compared to standard settings (BR ≤ 1). Furthermore, we investigate what the optimal BR depends on and conclude that it is more a property of the dataset than a dependence on the random forest hyperparameters. Finally, we develop a binary classifier to predict whether the optimal BR is ≤ 1 or > 1 for a given dataset, achieving between 81.88% and 88.81% accuracy, depending on the experiment configuration. The code is available at: <placeholder>.

1 INTRODUCTION

Random forest (RF) algorithm, introduced by Breiman (2001), is an ensemble of decision trees (DTs) that collectively make decisions using either majority or soft voting. RF reduces variance, sometimes at the cost of slightly increasing bias, by introducing two sources of randomness. The first is the use of distinct subsets of features when selecting the best split at each node of the trees. The second is training each tree on a subset of observations drawn with replacement from the original training set, i.e., a bootstrap sample.

In this study, we analyze the bootstrap rate (BR), an RF hyperparameter that controls the training process and consequently affects the model's performance. BR is defined as the ratio of the number of observations in each bootstrap sample to the total number of training instances. In the literature, this parameter is also referred to as the sample rate, subsample size, bootstrap size ratio, or bag size. In his original work, Breiman (2001) used BR $= 1$. However, lower values have also been successfully applied (Martínez-Muñoz & Suárez, 2010; Adnan, 2014). When BR is low, each tree is trained on a more distinct subset of the data, which increases diversity among RF estimators. Naturally, the computational cost is reduced compared to BR $= 1$. On the other hand, the trees may become too weak, as they are trained on a relatively smaller portion of the data. For BR $= 1$, the expected fraction of unique observations from the entire dataset is 63.2%. When BR < 1, this fraction is even lower.

For BR $= 1$, we expect 36.8% of observations to be absent in each bootstrap sample. Intuitively, there is no obvious answer as to what would happen if BR > 1. A higher BR, on the one hand, causes subsets to be less diverse, but on the other hand, it includes more unique observations (i.e., more information) in each sample. We found this problem worth investigating. To our knowledge, Martínez-Muñoz & Suárez (2010) are the only ones who have analyzed BR > 1. However, they only considered BR = 1.2 and concluded that such parameterization is generally ineffective. In our work, we not only analyze BR $= 1.2$ (and lower) but also explore higher values of 2, 3, 4, and 5. Additionally, we extend the experimental setup to 18 RF configurations, compared to what appears

to be a single configuration (though this is not clearly specified) in the reference paper. Surprisingly, and in contrast to the findings of Martínez-Muñoz & Suárez (2010), we discover that BR > 1 often yields better results than conventional BR values in the range $(0, 1]$.

The primary contributions of this work can be summarized in four key points:

- To our knowledge, we are the first to analyze and shed light on what the optimal BR value depends on;
- To our knowledge, we are the first to suggest that testing BR > 1 is meaningful and often yields better results than the standard BR ≤ 1;
- We demonstrate that the optimal BR is only partially dependent on the RF configuration and is more a property of the dataset;
- We develop a binary classifier that, based on the class structure, predicts whether the optimal BR is ≤ 1 or > 1 for a given dataset, and achieves an accuracy between 81.88% and 88.81%, depending on the experimental configuration.

2 Related Literature

Probst et al. (2019), in their survey on RF tuning, point out several hyperparameters that are commonly targeted by researchers when optimizing RF. The number of trees, which is the most extensively explored RF hyperparameter, was analyzed by Oshiro et al. (2012); Scornet (2017); Probst & Boulesteix (2018). The optimization of the number of attributes to consider when looking for the best split was addressed by Bernard et al. (2009); Goldstein et al. (2011). Additionally, Scornet (2017); Duroux, Roxane & Scornet, Erwan (2018) analyzed maximum tree depth.

We found the BR hyperparameter to be underresearched. Probst et al. (2019) consider it to have a minor influence on RF performance, while simultaneously stating that it is often worth tuning. Duroux, Roxane & Scornet, Erwan (2018) claim that due to the complexity of RFs, conducting a thorough theoretical analysis is challenging. As a result, most studies either overlook bootstrapping entirely (Biau et al., 2008; Ishwaran & Kogalur, 2010; Denil et al., 2013) or focus on simplified versions of RF, such as median forests (Scornet, 2017; Duroux, Roxane & Scornet, Erwan, 2018).

The study most relevant to our research was conducted by Martínez-Muñoz & Suárez (2010). First, it is the only work we found that analyzed BR > 1, although it is limited to a BR value of 1.2. Second, they examine how RF performance depends on BR. Among the 30 datasets analyzed, four types of BR curves showing the relationship between BR and classification error were identified. However, the analysis is limited to just one RF configuration and does not explore why the optimal BR may differ significantly between datasets—there is no insight provided as to why a particular curve shape is associated with a given dataset.

3 Experiment Configuration

Experiments were conducted on 36 diverse datasets, which underwent the following preprocessing steps: all duplicates and rows with classes occurring only once were removed. Columns with a single unique value were also dropped. Missing values in categorical features were replaced with a new category, while missing values in numerical attributes were imputed with the column mean. Finally, one-hot encoding of categorical attributes was applied before standardizing all features. Table 3 in Appendix A presents the characteristics of the datasets after the preprocessing. Our experiments include all 30 datasets used by Martínez-Muñoz & Suárez (2010) and six additional ones.

The following hyperparameters (along with BR) are considered to be the most important for RF performance (Scornet, 2017; Probst et al., 2019; Zhu et al., 2022): number of trees (nt); parameters controlling the size of the trees: maximum tree depth (md), the minimum number of instances required to split an internal node (mn), the minimum count of observations necessary to constitute a leaf node (ml); function measuring the quality of a split (qs); number of attributes to consider when looking for the best split (nf).

As the base values for these hyperparameters, we adopted the defaults from the scikit-learn 1.1.3 Python package: $nt = 100$, $md =$ None (no depth limit), $qs =$ "gini" (Gini impurity), $mn = 2$, ml

$= 1$, $nf =$ "sqrt" (square root of the number of features). We denote such a model as RF(base). Altogether, we tested RF(base) and 17 other configurations resulting from the following modifications of each single hyperparameter in RF(base):

- RF(nt_200), RF(nt_500): number of trees equals 200 or 500, respectively;
- RF(md_10), RF(md_15), RF(md_20), RF(md_25): maximum depth of a tree equals 10, 15, 20, or 25, respectively;
- RF(qs_ent): split quality is measured using Shannon entropy (information gain);
- RF(mn_3), RF(mn_4), RF(mn_6), RF(mn_8): minimum number of observations required to split an internal node is equal to 3, 4, 6, or 8, respectively;
- RF(ml_2), RF(ml_3), RF(ml_4), RF(ml_5): minimum number of instances per leaf is 2, 3, 4, or 5, respectively;
- RF(nf_log), RF(nf_all): number of features considered in a node split equals the logarithm with base 2 of the number of attributes or all features are taken into account, respectively.

The following BRs were tested: 0.2, 0.4, 0.6, 0.8, 1.0, 1.2 (as analyzed by Martínez-Muñoz & Suárez (2010)), 2.0, 3.0, 4.0, and 5.0. For each configuration, 2-fold stratified cross-validation, repeated 200 times, was applied, yielding 400 results.

4 RESULTS

For each dataset, we searched for the pair of RF configuration and BR that yielded the highest classification accuracy. Table 1 presents these results. Detailed results, including the mean accuracy and standard deviation for individual RF configurations and datasets, are provided in Appendix B.

Statistical significance. The main observation is that BR > 1 constituted the best setup in 20 out of 36 datasets. To further compare standard BRs (BR ≤ 1, first group) with those greater than one (second group), we performed a paired t-test (with the alternative hypothesis that the first sample has a greater mean than the second one) on the results of the dataset winner (best performing configuration) and results from all configurations with the other BR group. So, if the best classification accuracy was achieved by RF with BR ≤ 1, we compared these results with all results related to configurations with BR > 1, and vice versa. The last column of the table shows the maximum p-value among all t-tests for each dataset. We analyzed several significance levels: 0.1, 0.05, 0.01, 0.001, 0.0001, and 0.00001. Considering only conclusive results (i.e., p-values lower than the specified significance level), the difference in the number of datasets with the best related model with BR > 1 versus those with BR ≤ 1 amounted to 5, 2, -2, -4, -2, and 0, respectively. This indicates that, depending on the chosen significance level, the number of datasets with the optimal solution involving BR ≤ 1 is roughly comparable to those with BR > 1.

Number of winning configurations. Among the 18 analyzed RF configurations, only seven achieved the highest classification accuracy in at least one dataset: RF(nt_500) (20 datasets), RF(qs_ent) (5 datasets), RF(ml_5) (4 datasets), RF(mn_8) (3 datasets), RF(ml_4) (2 datasets), RF(mn_4) (1 dataset), and RF(nf_all) (1 dataset). Further analysis will concentrate on these setups.

Frequence of winning BRs. Fig. 1 depicts the frequency of winning BRs, both globally and for each RF parameter setting. The histogram related to RF(nt_500) is the most similar to the global one, as this model achieved the best score in 20 out of 36 datasets. For RF(ml_4) and RF(ml_5), models that restrictively control the size of the tree, BR > 1 constituted the best setup for as many as 26 datasets. It stems from the fact that, in many cases, a low number of training instances combined with a relatively high minimum number of samples required to create a leaf led to underfitted trees. Thus, high BR served as a remedy, enabling the construction of more complex models. RF(nf_all) exhibited different behavior compared to the other models. The higher the BR, the less frequently it was optimal. The key sources of diversity among the individual trees are the distinct subsets of attributes to consider when looking for the best split in each node, along with the unique bootstrap sample used in training. When all features are analyzed in a node splitting, the first source of diversity ceases to exist. Thus, to maintain an overall level of diversity, RF(nf_all) preferred lower BRs,

Table 1: Classification results. The consecutive columns present the dataset name, the optimal RF configuration, the achieved accuracy, the best BR, and the p-value from the conducted t-test.

Dataset	Best model	Acc. [%]	Bootstrap rate	p-value
Abalone	RF(ml_5)	26.801	0.2	$< 10^{-6}$
Adult	RF(ml_5)	86.484	4.0	$< 10^{-6}$
Arrhythmia	RF(nf_all)	76.161	1.2	0.305022
Audiology (Standardized)	RF(mn_8)	75.338	5.0	0.013121
Australian Credit Approval	RF(nt_500)	87.225	0.6	0.132623
Balance Scale	RF(nt_500)	85.972	0.2	$< 10^{-6}$
Breast Cancer Wisc. (Diag.)	RF(qs_ent)	95.898	5.0	$< 10^{-6}$
Breast Cancer Wisc. (Orig.)	RF(nt_500)	95.506	0.4	0.001910
Congressional Voting Rec.	RF(mn_8)	94.795	2.0	0.029394
Echocardiogram	RF(ml_5)	73.113	2.0	0.035933
Ecoli	RF(nt_500)	85.835	0.6	0.000097
German Credit Data	RF(nt_500)	75.467	1.2	0.079419
Glass Identification	RF(qs_ent)	75.596	2.0	0.002702
Heart	RF(ml_4)	83.324	0.2	0.000004
Hepatitis	RF(nt_500)	84.726	0.4	0.000644
Horse Colic	RF(nt_500)	86.516	1.0	0.485986
Image Segmentation (Stat.)	RF(qs_ent)	97.133	5.0	$< 10^{-6}$
Ionosphere	RF(nt_500)	93.254	1.2	0.192406
Iris	RF(mn_4)	95.232	0.4	0.105220
Labor Relations	RF(nt_500)	93.608	1.2	0.004194
Liver Disorders	RF(ml_4)	59.714	0.2	$< 10^{-6}$
Optical Recognition (Digits)	RF(nt_500)	97.413	4.0	$< 10^{-6}$
Parkinsons	RF(nt_500)	89.306	5.0	$< 10^{-6}$
Pima Indians Diabetes	RF(nt_500)	76.344	0.2	0.000018
Sonar, Mines vs. Rocks	RF(qs_ent)	81.627	4.0	$< 10^{-6}$
Soybean (Large)	RF(mn_8)	92.712	4.0	$< 10^{-6}$
Tic-Tac-Toe Endgame	RF(nt_500)	97.264	5.0	0.021006
Thyroid Disease	RF(qs_ent)	95.840	1.2	0.059261
Vehicle Silhouettes	RF(nt_500)	74.583	5.0	0.001911
Vowel Recognition	RF(nt_500)	92.285	3.0	$< 10^{-6}$
Wine	RF(nt_500)	97.809	1.2	0.072172
Ringnorm	RF(nt_500)	92.717	0.6	$< 10^{-6}$
Threenorm	RF(nt_500)	80.050	0.4	0.000654
Twonorm	RF(nt_500)	96.002	0.2	$< 10^{-6}$
Waveform	RF(nt_500)	86.165	0.2	$< 10^{-6}$
LED Display Domain	RF(ml_5)	66.590	1.0	$< 10^{-6}$

which created more varied sets of samples drawn and made the trees less correlated. Looking at the BR histograms, extreme BR values (0.2 and 5.0) constituted the best solutions, both overall and for all analyzed RF configurations, the greatest number of times (the highest bar in each histogram corresponds either to 0.2 or 5.0). This suggests that the optimal BR may often be lower than 0.2 or higher than 5.0, indicating that even a broader range should be tested when tuning RF. Finally, BR $= 1$, defined in the original formulation of the bootstrapping procedure and the most frequently used value, performed relatively poorly. Overall, it was optimal for only two datasets. When analyzing individual RF configurations, for three of them, BR $= 1$ was not able to win even in one dataset. Averaging over all seven parameter settings, it was optimal for only 1.43 out of 36 datasets. Interestingly, adjacent to 1, the nonstandard BR $= 1.2$ was, with the exception of RF(nf_all), always better, often substantially.

Individual dataset analysis. Fig. 2 illustrates the relationship between the performance and BR for the analyzed RF configurations across a selected group of diverse datasets. Charts for the remaining datasets are provided in Appendix C. Our first observation is that RF(nf_all) behaves differently

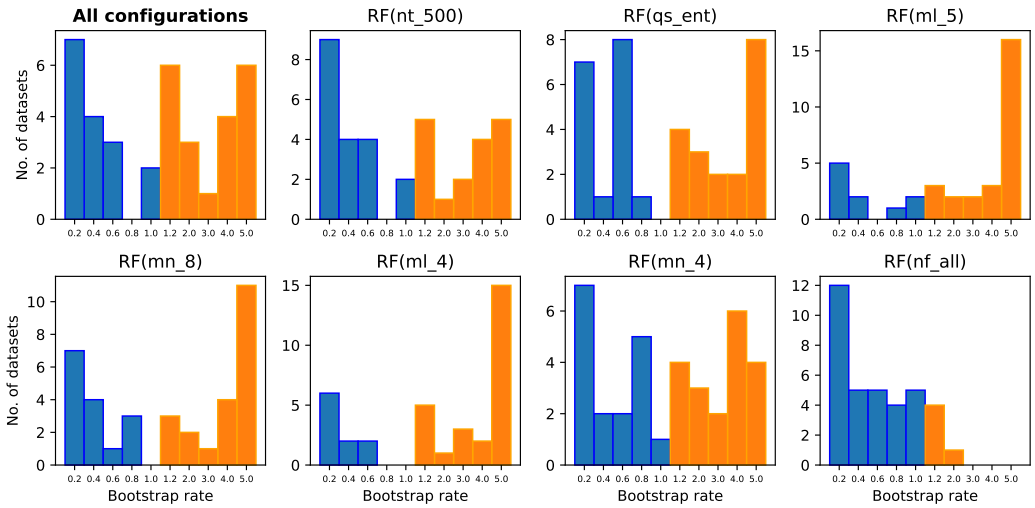

Figure 1: Distribution of winning BR across all RF configurations (top left) and among individual RF parameterizations.

from the other models. In almost all cases, it reaches optimal accuracy with a lower (or equal) BR compared to other RFs. This observation is consistent with the trends shown in Fig. 1 and the explanation provided in the previous paragraph. In most cases, the best accuracy achieved by RF(nf_all) is substantially worse than that of the other models, and after reaching the optimum, its performance declines rapidly. There are several datasets for which RF(nf_all) performs well. It achieved the best accuracy across all models on the Arrhythmia dataset and was comparable to the best on Audiology (Standardized), Tic-Tac-Toe Endgame, Pima Indians Diabetes, and Iris. The high performance of RF(nf_all) is undoubtedly related to the characteristics of the features, e.g., the abovementioned Arrhythmia has the highest number of features among all datasets. However, the relationship is more complex for the other four datasets. We hypothesize that the importance of features needs to be further assessed to gain deeper insights. Presumably, RF(nf_all) will perform well on datasets with a high proportion of insignificant or less significant features, as it may avoid building trees primarily based on these features.

Typical BR curve shapes. All RF configurations other than RF(nf_all) are generally similar in terms of the characteristics of their BR curves. We identified three categories that describe how the set of curves appears:

(a) In the first and most common pattern, all curves increase to at least BR $= 1.2$, indicating that the optimal BR is at least 1.2. The curves then either continue to rise (usually more smoothly)/reach a plateau (first subpattern) or they oscillate/gradually decrease (second subpattern). The first subpattern can be observed in the Arrhythmia, Audiology (Standardized), Parkinsons, Breast Cancer Wisc. (Diag.), Optical Recognition (Digits), Ionosphere, Image Segmentation (Stat.), Sonar, Mines vs. Rocks, Soybean (Large), Tic-Tac-Toe Endgame, Vowel, and Recognition datasets. The second subpattern is seen in the Wine, German Credit Data, Glass Identification, Labor Relations, Thyroid Disease, Vehicle Silhouettes, and Congressional Voting Rec. datasets.

(b) In the second pattern, all curves either decrease from the very beginning (BR $= 0.2$) or rise to a BR in the range $[0.4, 1.0]$ and then decline. The overall shape of the curves may be fairly smooth, as seen in the Abalone, Balance Scale, Breast Cancer Wisc. (Orig.), Heart, Liver Disorders, Twonorm, Waveform, and LED Display Domain datasets, or it may exhibit some irregularities, as observed in the Iris and Pima Indians Diabetes datasets.

(c) The third pattern is a mixture of the first and second patterns. Curves associated with some RF configurations, mainly RF(ml_4) and RF(ml_5), behave similarly to those in the first pattern, while others resemble the curves seen in the second pattern. This third pattern is present in the Adult, Aus-

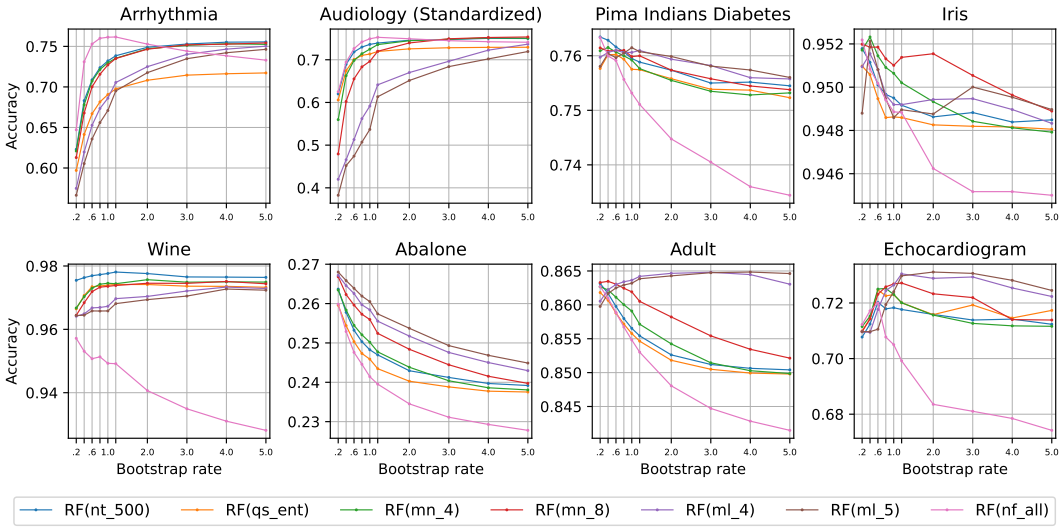

Figure 2: Characteristics of bootstrap rate curves for selected datasets.

tralian Credit Approval, Ecoli, Hepatitis, Ringnorm, Threenorm, Horse Colic, and Echocardiogram datasets. In the case of the last two, some additional irregularities in the BR curves may be observed.

The main observation from the above analysis is that BR curves associated with all RF configurations, except RF(nf_all), are fairly consistent. The first and second patterns, within which all curves exhibit similar behavior, were observed in 28 out of 36 datasets. This leads to the conclusion that the optimal BR is merely dependent on RF parameterization and is closely related to the dataset.

Naturally, the procedure for testing high BR values follows a typical 'no free lunch' scenario—while we may find RF configuration yielding better results, it comes at the cost of slower execution, as it involves sampling more observations and building trees on a larger number of instances. We did not analyze issues related to time performance, which may represent potential direction for further research.

5 Towards Understanding the Optimal Bootstrap Rate

Higher level approaches. While searching for the reasons why the BR curve differs so significantly between datasets, we began with analyzing the general properties of these datasets, such as the number of features (divided into continuous and binary) and the number of training instances. We also created new features reflecting interactions by applying arithmetic operations to the aforementioned attributes. However, neither approach helped us to understand the problem better. Next, we took a more local approach and examined whether the BR curve was associated with the number of clusters present in the data. Unfortunately, this research direction was also inconclusive. In the meantime, we observed that even small changes in the data could lead to significant changes in the shape of the BR curve and the optimal value of BR. Fig. 3 provides an example. This observation prompted us to go even more local and analyze the neighborhood of individual instances.

Lower level approaches. In brief, RF is composed of DTs that cut the feature hyperspace into decision regions defined by the path leading from the root to the corresponding leaf. In a single tree, the prediction for a sample located in a particular leaf region is based on the majority class of the instances that reached that leaf during training. This means that the neighbors (specifically, their classes) of the predicted instance affect the predicted label. The same applies to RF, as it performs majority voting on predictions made by the component DTs. To analyze the structure of neighbors in each dataset, we standardized all continuous features and mapped all binary attributes to -1 and 1. We employed the Manhattan metric, which considers the distance along each feature (axis) independently, to measure the distance between observations. The Manhattan distance is generally

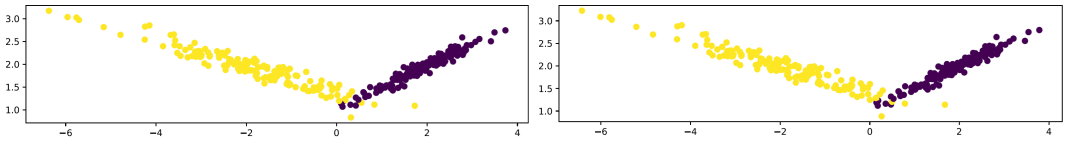

(a) $class\_sep = 1.95$ (b) $class\_sep = 2.0$

Figure 3: An example illustrating how even small differences in the data can significantly affect the optimal BR value. Both figures (a) and (b) depict synthetically generated data using scikit-learn's $make\_classification$ method with the following parameters: $n\_samples = 300$, $n\_features = 2$, $n\_classes = 2$, $n\_clusters\_per\_class = 1$, and $random\_state = 1$. The only difference is the value of the $class\_sep$ parameter, which controls the separation between the classes. In (a), it is set to 1.95, while in (b), it is 2.0. As a result of this slight difference, the optimal BR in (a) equals 5.0, while in (b), it amounts to 0.2. All other parameters of the $make\_classification$ method remain at their default values.

a good choice in the context of a DT (and RF), which also defines a decision boundary that, at any moment, moves along only one feature.

Let us introduce the notation k_l, which is the number of observations for which, among k nearest neighbors, l samples belong to the same class as the considered instance. Intuitively, high k_l values for low l, relative to k, indicate inhomogeneity in the data and possibly a relatively high number of outliers. For each dataset, we calculated the k_l statistics for $k \in \{1, 2, \ldots, 10\}$ and $l \in \{0, \ldots, k\}$ for each k. Then, we performed normalization so that for each k, the sum k_0, ..., k_k equaled 100, making those values comparable between datasets of varying sizes.

For each k_l and each RF's optimal BR, including the overall best, we calculated the Spearman rank-order correlation coefficient. Table 2 presents the results for $k \in \{1, 2, \ldots, 6\}$. Our first observation is that the overall best BR is always positively correlated with k_k. The highest correlation corresponds to $k = 1$, 2, 3, after which it gradually decreases. Second, for each k_l where $l \neq k$, the correlation is negative; the lower l is, the stronger the correlation becomes in terms of absolute value. This means that the optimal BR for inhomogeneous datasets (high k_l values for low l) tends to be lower than for uniform datasets (high k_l values for l close to k). A low BR leads to ambiguous observations being drawn less frequently. Therefore, fewer decision trees have leaves affected by such instances, and the remaining RF trees may mitigate incorrect decisions in the majority voting scheme. Conversely, for more uniform data, we hypothesize that a higher BR yields better results because it creates a bootstrap sample with more unique instances, thereby providing more information while maintaining diversity through varying the number of occurrences of these instances. Finally, an excessively high BR does not yield good results because it reduces diversity; as a consequence of the law of large numbers, the number of occurrences of individual observations converges towards each other.

Optimal BRs related to individual RF configurations share properties similar to those of the best overall BR. For all k, the correlation between k_k and the optimal BR is positive, gradually decreasing after 2_2 (or 1_1 in the case of RF(nf_all)). The rest of the k_l values ($l \neq k$), for $k \leq 5$, are negative, with some exceptions for 5_4. The trend between k_0 and k_k is generally upward, but unlike the best overall BR, it is non-monotonic. RF(nf_all) exhibits this behavior as well, but the range of k_l values is visibly narrower, and some irregularity occurs for $k = 5$.

For the increasing k, starting from $k = 6$, the general ascending trend from k_0 to k_k is maintained. However, the range $[k\_0, k\_k]$ narrows, the changes are not perfectly monotonic, and more positive values, other than k_k, appear. We suppose that considering $k > 5$ becomes too general (causing the above irregularities) but still reflects the uniformity of the data (hence, an overall trend is maintained).

The absolute values of the correlation coefficients are not high. For the overall best BR, the highest Spearman rank-order correlation coefficient amounts to 0.330. This is because the function modeling the optimal BR is complex and not dependent on just one predictor. We found two ways to build attributes that are more highly correlated with the target. The first is by multiplying each feature (k_l) by the number of classes in a particular dataset. Intuitively, the higher the number of classes,

Table 2: Spearman rank-order correlation coefficient between k_l and the best BR—overall (second column) and respective RF configurations (columns 3–9).

k_l	Best RF	nt_500	qs_ent	ml_5	mn_8	ml_4	mn_4	nf_all
1_0	-0.311	-0.299	-0.345	-0.319	-0.312	-0.332	-0.387	-0.173
1_1	0.311	0.299	0.345	0.319	0.312	0.332	0.387	0.173
2_0	-0.292	-0.252	-0.292	-0.263	-0.258	-0.280	-0.354	-0.156
2_1	-0.252	-0.264	-0.298	-0.255	-0.241	-0.277	-0.317	-0.164
2_2	0.330	0.301	0.347	0.320	0.320	0.332	0.379	0.163
3_0	-0.264	-0.258	-0.275	-0.242	-0.263	-0.256	-0.350	-0.139
3_1	-0.250	-0.238	-0.311	-0.264	-0.250	-0.292	-0.331	-0.142
3_2	-0.239	-0.213	-0.230	-0.164	-0.163	-0.192	-0.261	-0.183
3_3	0.323	0.280	0.341	0.307	0.294	0.320	0.365	0.151
4_0	-0.292	-0.266	-0.278	-0.254	-0.268	-0.258	-0.351	-0.134
4_1	-0.261	-0.233	-0.283	-0.255	-0.249	-0.274	-0.325	-0.159
4_2	-0.213	-0.208	-0.264	-0.209	-0.179	-0.235	-0.280	-0.147
4_3	-0.114	-0.116	-0.134	-0.031	-0.056	-0.067	-0.158	-0.090
4_4	0.299	0.261	0.319	0.286	0.269	0.301	0.346	0.146
5_0	-0.238	-0.221	-0.218	-0.198	-0.185	-0.217	-0.285	-0.099
5_1	-0.227	-0.178	-0.224	-0.183	-0.201	-0.205	-0.267	-0.034
5_2	-0.223	-0.232	-0.298	-0.230	-0.220	-0.264	-0.321	-0.134
5_3	-0.204	-0.148	-0.181	-0.114	-0.113	-0.143	-0.211	-0.127
5_4	-0.084	-0.027	-0.035	0.096	0.056	0.055	-0.058	0.003
5_5	0.302	0.244	0.301	0.269	0.245	0.285	0.318	0.125
6_0	-0.213	-0.186	-0.170	-0.165	-0.149	-0.182	-0.251	-0.080
6_1	-0.156	-0.134	-0.183	-0.127	-0.165	-0.156	-0.223	0.031
6_2	-0.234	-0.239	-0.292	-0.225	-0.214	-0.261	-0.328	-0.154
6_3	-0.158	-0.128	-0.199	-0.167	-0.136	-0.198	-0.213	-0.015
6_4	-0.109	-0.041	-0.062	0.039	0.039	0.008	-0.086	-0.083
6_5	-0.013	0.030	-0.001	0.169	0.125	0.129	0.030	0.080
6_6	0.265	0.204	0.261	0.220	0.190	0.235	0.260	0.080

the lower the probability that outliers (ambiguous observations) from the same class, potentially forming a decision leaf in a tree, are drawn. Indeed, the correlation coefficients move upward. The negative ones become closer to zero or even turn positive. For example, for the overall best BR, 2_0, 3_2, and 4_3 increase from -0.292, -0.239, and -0.114 to -0.191, -0.041, and 0.038, respectively. Similarly, the positive values rise even higher. For instance, 2_2, 3_3, and 4_4 increase from 0.330, 0.323, and 0.299 to 0.456, 0.493, and 0.454, respectively.

The second way to create predictors with a higher correlation to the target is to introduce features that represent interactions between existing attributes k_l, where $k \in \{1, 2, \ldots, 10\}$ and $l \in \{0, \ldots, k\}$ for each k. More specifically, for all pairs of distinct features, we perform division, subtraction, multiplication, and addition (the first two in both directions). Additionally, each attribute is multiplied by itself and added to itself, creating two additional features. In this way, 12 620 new attributes are created. The features most positively correlated with the target are 9_2/2_0 (9_2 divided by 2_0), 10_2/3_0, and 10_2/4_0. The respective correlation coefficients are 0.607, 0.595, and 0.595.

Bootstrap rate prediction. To further assess how well the above set of attributes describes the problem, we used them (along with base k_l statistics) to build a binary classifier predicting whether the optimal BR across all RF configurations is ≤ 1 or > 1 for a given dataset. As in the main experiments, we tested all 18 RF configurations and 10 BR values. Due to the limited number of observations—each corresponding to one of 36 datasets—we performed Leave-Two-Out Cross-Validation in all possible variants, yielding 320 train-validation splits. Given the high dimensionality

(12 685 features), the initial results were poor. To address this, we reduced the number of input features to the k highest correlated with the target, with k ranging from 1 to 10, based on the absolute value of the Spearman rank-order coefficient, calculated separately for each run on the training instances. The best classification accuracy, averaged over all 320 runs, equaled 81.88% and was achieved by RF(nt_200) with BR $= 0.4$, using seven attributes.

Differences in classification accuracies between different BRs are sometimes marginal. Therefore, another experiment was conducted, this time focusing only on observations with undisputed labels. We assumed these are datasets for which the corresponding p-value in Table 1 is at most 0.01. A total of 24 observations met this condition. The remaining experimental configuration was the same as in the previous experiment. Leave-Two-Out Cross-Validation was performed on all possible 143 train-validation splits. The highest accuracy, 88.81%, was achieved by RF(nf_all) with BR $= 0.8$, using only three features.

In both of the above experiments, the number of training instances was low: 36 and 24, respectively. We believe that a simple increase in these numbers may lead to further improvements in performance. Additionally, both datasets were well-balanced, with the majority class constituting 55.56% and 54.17%, respectively. Thus, we conclude that the proposed attributes, which enabled us to achieve accuracies of 81.88% and 88.81%, can be considered as effective descriptors of the analyzed problem.

6 Conclusions and Future Work

In this paper, we analyze the BR hyperparameter in RF. To the best of our knowledge, this work is the first to shed light on what the optimal BR value depends on and to demonstrate that it is often greater than 1, thus exceeds the standard values within the $(0, 1]$ range. We also show that the optimal BR value is largely independent of the other hyperparameters of the RF. In fact, most RF configurations are highly correlated in terms of the BR curve, which makes the optimal BR value more of a property of the dataset.

Our main conclusion stating that BR > 1 often yields superior results and is worth considering contradicts the findings of the baseline reference paper (Martínez-Muñoz & Suárez, 2010). We identify two main reasons for this. First, the authors of (Martínez-Muñoz & Suárez, 2010) stopped their analysis at BR $= 1.2$ and did not explore higher values. Second, they most likely tested only one RF configuration. In fact, they did not provide any details regarding the RF hyperparameters, other than stating that the ensemble was composed of 200 unpruned CART trees (Breiman et al., 1984).

Prediction of the optimal BR value is a complex task, highly dependent on the local class structure. In this work, we propose to calculate k_l statistics, which reflect the number of observations from the same class as the instances considered in their neighborhood and use them to calculate the correlations with the optimal BR value. While this approach works generally well, we believe that it cas still be improved through describing the local class structure in a different, possibly more precise way.

Considering nearest neighbors assumes that the analyzed observation is located at the center of the decision regions and that these regions form a hypercube, meaning all decision hyperplanes are equally distant from the analyzed sample. This is a simplification, as in real-world scenarios, the range of features corresponding to a decision subspace is usually unequal, and no point lies exactly at the center of all feature ranges. Therefore, analyzing an instance's neighborhood by sampling each feature range to reflect the different decision subspaces to which a particular instance may belong may be a viable approach.

Another research direction worth exploring is to extend k_l to more detailed statistics that specify the number of neighbors from each individual class. k_l can be interpreted as the number of instances for which, among the k nearest neighbors, $k - l$ observations belong to classes other than the one under consideration. We believe that the distribution of these classes may be useful in predicting the optimal BR. The more uniform the distribution (with no dominant class), the easier it is for an ambiguous example to outvote the correct class in a majority or soft voting scheme.

Finally, we examined three well-established ML libraries: scikit-learn, Weka, and H2O.ai. In all of them, values of the BR hyperparameter greater than one are disabled in their RF implementations. Based on our findings, we recommend that the developers of ML libraries consider making this feature available.

REFERENCES

Md Nasim Adnan. Improving the Random Forest Algorithm by Randomly Varying the Size of the Bootstrap Samples. In *Proceedings of the 2014 IEEE 15th International Conference on Information Reuse and Integration, IEEE IRI 2014*, pp. 303–308, 08 2014.

Simon Bernard, Laurent Heutte, and Sébastien Adam. Influence of Hyperparameters on Random Forest Accuracy. In *Multiple Classifier Systems*, pp. 171–180. Springer Berlin Heidelberg, 2009.

Gérard Biau, Luc Devroye, and Gábor Lugosi. Consistency of Random Forests and Other Averaging Classifiers. *Journal of Machine Learning Research*, 9(66):2015–2033, 2008.

Leo Breiman. Arcing Classifiers. *The Annals of Statistics*, 26(3):801–824, 1998.

Leo Breiman. Random Forests. *Machine Learning*, 45:5–32, 2001.

Leo Breiman, Jerome Friedman, Charles J. Stone, and Richard A. Olshen. *Classification and Regression Trees*. Taylor & Francis, 1984.

Misha Denil, David Matheson, and Nando Freitas. Consistency of Online Random Forests. In *Proceedings of the 30th International Conference on Machine Learning*, volume 28, pp. 1256–1264. PMLR, 2013.

Duroux, Roxane and Scornet, Erwan. Impact of subsampling and tree depth on random forests. *ESAIM: PS*, 22:96–128, 2018.

Benjamin A Goldstein, Eric C Polley, and Farren B. S. Briggs. Random Forests for Genetic Association Studies. *Statistical Applications in Genetics and Molecular Biology*, 10(1), 2011.

Hemant Ishwaran and Udaya B. Kogalur. Consistency of random survival forests. *Statistics & Probability Letters*, 80(13):1056–1064, 2010.

Markelle Kelly, Rachel Longjohn, and Kolby Nottingham. The UCI Machine Learning Repository. `https://archive.ics.uci.edu`, 2023. Accessed: 2024-07-11.

Gonzalo Martínez-Muñoz and Alberto Suárez. Out-of-bag estimation of the optimal sample size in bagging. *Pattern Recognition*, 43(1):143–152, 2010.

Thais Mayumi Oshiro, Pedro Santoro Perez, and José Augusto Baranauskas. How Many Trees in a Random Forest? In *Machine Learning and Data Mining in Pattern Recognition*, pp. 154–168. Springer Berlin Heidelberg, 2012.

Philipp Probst and Anne-Laure Boulesteix. To Tune or Not to Tune the Number of Trees in Random Forest. *Journal of Machine Learning Research*, 18(181):1–18, 2018.

Philipp Probst, Marvin N. Wright, and Anne-Laure Boulesteix. Hyperparameters and tuning strategies for random forest. *WIREs Data Mining and Knowledge Discovery*, 9, 2019.

Erwan Scornet. Tuning parameters in random forests. *ESAIM: Procs*, 60:144–162, 2017.

Ningyuan Zhu, Chaoyang Zhu, Liang Zhou, Yayun Zhu, and Xiaojuan Zhang. Optimization of the Random Forest Hyperparameters for Power Industrial Control Systems Intrusion Detection Using an Improved Grid Search Algorithm. *Applied Sciences*, 12(20), 2022.

Appendices

A DATASETS

Table 3: Dataset characteristics. The subsequent columns refer to the dataset name, the number of numerical and binary features, the number of observations, and the count of classes. The first 31 datasets presented in the table come from the UCI Machine Learning Repository (Kelly et al., 2023). The next four are from Breiman (1998), and the last one is from Breiman et al. (1984).

Dataset	Numerical features	Binary features	Observations	Classes
Abalone	7	3	4172	23
Adult	6	85	48790	2
Arrhythmia	194	64	420	12
Audiology (Standardized)	0	89	171	18
Australian Credit Approval	6	32	690	2
Balance Scale	0	20	625	3
Breast Cancer Wisc. (Diag.)	30	0	569	2
Breast Cancer Wisc. (Orig.)	9	0	449	2
Congressional Voting Rec.	0	48	342	2
Echocardiogram	6	1	62	2
Ecoli	5	1	336	8
German Credit Data	6	53	1000	2
Glass Identification	9	0	213	6
Heart	7	13	270	2
Hepatitis	6	27	148	2
Horse Colic	7	140	368	2
Image Segmentation (Stat.)	18	0	2086	7
Ionosphere	32	1	350	2
Iris	4	0	149	3
Labor Relations	8	29	57	2
Liver Disorders	5	0	341	2
Optical Recognition (Digits)	61	0	1797	10
Parkinsons	22	0	195	2
Pima Indians Diabetes	8	0	768	2
Sonar, Mines vs. Rocks	60	0	208	2
Soybean (Large)	0	132	631	19
Tic-Tac-Toe Endgame	0	27	958	2
Thyroid Disease	5	0	215	3
Vehicle Silhouettes	18	0	845	4
Vowel Recognition	10	0	990	11
Wine	13	0	178	3
Ringnorm	20	0	300	2
Threenorm	20	0	300	2
Twonorm	20	0	300	2
Waveform	21	0	300	3
LED Display Domain	0	24	200	10

B Detailed Results

Table 4: Classification accuracy (mean ± standard deviation) for the Abalone dataset.

BR	RF(nt_500)	RF(qs_ent)	RF(mn_4)	RF(mn_8)	RF(ml_4)	RF(ml_5)	RF(nf_all)
0.2	26.368 ± 0.719	25.959 ± 0.753	26.345 ± 0.759	26.682 ± 0.766	26.718 ± 0.711	26.801 ± 0.703	25.984 ± 0.799
0.4	25.777 ± 0.744	25.439 ± 0.769	25.835 ± 0.764	26.229 ± 0.754	26.457 ± 0.746	26.584 ± 0.714	25.290 ± 0.766
0.6	25.323 ± 0.741	25.032 ± 0.750	25.447 ± 0.748	25.963 ± 0.774	26.256 ± 0.750	26.388 ± 0.740	24.761 ± 0.781
0.8	25.031 ± 0.746	24.732 ± 0.780	25.206 ± 0.767	25.729 ± 0.747	25.970 ± 0.775	26.190 ± 0.803	24.458 ± 0.777
1.0	24.825 ± 0.750	24.588 ± 0.719	25.017 ± 0.762	25.595 ± 0.762	25.840 ± 0.775	26.050 ± 0.730	24.142 ± 0.731
1.2	24.696 ± 0.726	24.346 ± 0.720	24.773 ± 0.721	25.243 ± 0.761	25.553 ± 0.735	25.738 ± 0.770	23.953 ± 0.724
2.0	24.294 ± 0.752	24.027 ± 0.726	24.383 ± 0.751	24.840 ± 0.768	25.173 ± 0.771	25.373 ± 0.797	23.452 ± 0.776
3.0	24.123 ± 0.747	23.883 ± 0.739	24.038 ± 0.776	24.445 ± 0.773	24.758 ± 0.739	24.932 ± 0.753	23.112 ± 0.814
4.0	23.970 ± 0.710	23.775 ± 0.714	23.861 ± 0.740	24.154 ± 0.738	24.502 ± 0.772	24.686 ± 0.753	22.930 ± 0.787
5.0	23.918 ± 0.725	23.753 ± 0.760	23.806 ± 0.723	23.972 ± 0.733	24.295 ± 0.713	24.489 ± 0.800	22.779 ± 0.835

Table 5: Results for the Adult dataset.

BR	RF(nt_500)	RF(qs_ent)	RF(mn_4)	RF(mn_8)	RF(ml_4)	RF(ml_5)	RF(nf_all)
0.2	86.315 ± 0.151	86.182 ± 0.152	86.266 ± 0.146	86.329 ± 0.152	86.053 ± 0.160	85.977 ± 0.157	86.270 ± 0.150
0.4	86.168 ± 0.151	86.068 ± 0.154	86.220 ± 0.144	86.347 ± 0.146	86.224 ± 0.155	86.167 ± 0.157	86.098 ± 0.154
0.6	85.977 ± 0.153	85.879 ± 0.157	86.112 ± 0.152	86.305 ± 0.146	86.300 ± 0.154	86.250 ± 0.152	85.886 ± 0.160
0.8	85.798 ± 0.159	85.717 ± 0.165	86.002 ± 0.158	86.245 ± 0.157	86.341 ± 0.154	86.292 ± 0.153	85.673 ± 0.168
1.0	85.654 ± 0.156	85.576 ± 0.157	85.908 ± 0.150	86.192 ± 0.150	86.363 ± 0.151	86.319 ± 0.155	85.482 ± 0.171
1.2	85.542 ± 0.157	85.464 ± 0.155	85.715 ± 0.158	86.052 ± 0.152	86.420 ± 0.152	86.385 ± 0.155	85.302 ± 0.171
2.0	85.261 ± 0.157	85.182 ± 0.158	85.424 ± 0.156	85.822 ± 0.153	86.465 ± 0.153	86.428 ± 0.157	84.805 ± 0.174
3.0	85.120 ± 0.154	85.049 ± 0.158	85.145 ± 0.157	85.542 ± 0.160	86.481 ± 0.153	86.475 ± 0.156	84.471 ± 0.192
4.0	85.063 ± 0.157	84.993 ± 0.157	85.028 ± 0.162	85.344 ± 0.154	86.447 ± 0.156	86.484 ± 0.155	84.284 ± 0.202
5.0	85.041 ± 0.157	84.979 ± 0.163	84.986 ± 0.163	85.214 ± 0.159	86.305 ± 0.156	86.462 ± 0.151	84.148 ± 0.211

Table 6: Results for the Arrhythmia dataset.

BR	RF(nt_500)	RF(qs_ent)	RF(mn_4)	RF(mn_8)	RF(ml_4)	RF(ml_5)	RF(nf_all)
0.2	62.300 ± 1.482	59.704 ± 1.396	62.098 ± 1.578	61.287 ± 1.432	57.487 ± 0.825	56.637 ± 0.439	64.712 ± 1.938
0.4	68.310 ± 1.629	64.137 ± 1.667	67.794 ± 1.825	66.781 ± 1.821	61.971 ± 1.519	60.544 ± 1.315	73.096 ± 2.006
0.6	70.875 ± 1.652	66.696 ± 1.631	70.719 ± 1.837	70.010 ± 1.815	65.270 ± 1.722	63.580 ± 1.615	75.290 ± 1.896
0.8	72.371 ± 1.683	68.155 ± 1.724	72.150 ± 1.771	71.561 ± 1.862	67.346 ± 1.845	65.598 ± 1.804	75.999 ± 1.944
1.0	73.208 ± 1.767	69.061 ± 1.656	72.975 ± 1.874	72.714 ± 1.928	68.610 ± 1.788	67.092 ± 1.843	76.130 ± 1.929
1.2	73.844 ± 1.792	69.758 ± 1.631	73.538 ± 1.945	73.505 ± 1.995	70.548 ± 1.793	69.507 ± 1.780	76.161 ± 1.949
2.0	74.887 ± 1.863	70.823 ± 1.605	74.706 ± 1.863	74.654 ± 1.939	72.496 ± 1.762	71.760 ± 1.868	75.277 ± 2.320
3.0	75.289 ± 1.910	71.452 ± 1.740	75.127 ± 1.972	75.193 ± 2.043	74.018 ± 1.969	73.482 ± 1.882	74.417 ± 2.534
4.0	75.518 ± 1.941	71.625 ± 1.742	75.327 ± 1.915	75.271 ± 1.865	74.660 ± 1.920	74.217 ± 1.858	73.840 ± 2.693
5.0	75.554 ± 1.831	71.726 ± 1.644	75.250 ± 1.948	75.427 ± 1.892	75.024 ± 1.807	74.637 ± 1.956	73.299 ± 2.860

Table 7: Results for the Audiology (Standardized) dataset.

BR	RF(nt_500)	RF(qs_ent)	RF(mn_4)	RF(mn_8)	RF(ml_4)	RF(ml_5)	RF(nf_all)
0.2	62.012 ± 3.483	60.583 ± 3.708	55.974 ± 3.811	47.936 ± 2.531	41.996 ± 4.582	38.258 ± 6.699	62.505 ± 3.902
0.4	68.927 ± 3.394	67.429 ± 3.510	66.274 ± 3.570	60.223 ± 3.823	46.573 ± 2.348	45.205 ± 2.154	69.445 ± 3.565
0.6	71.831 ± 3.390	70.062 ± 3.607	69.844 ± 3.525	65.517 ± 3.301	51.308 ± 3.124	47.432 ± 2.393	72.611 ± 3.894
0.8	72.977 ± 3.460	71.022 ± 3.488	71.411 ± 3.601	68.334 ± 3.502	56.200 ± 3.591	50.707 ± 3.160	74.181 ± 4.129
1.0	73.600 ± 3.529	71.338 ± 3.652	72.482 ± 3.604	69.635 ± 3.662	59.150 ± 3.630	53.672 ± 3.550	74.912 ± 4.221
1.2	73.914 ± 3.642	71.940 ± 3.598	73.553 ± 3.628	71.984 ± 3.495	64.130 ± 3.055	61.341 ± 3.446	75.257 ± 4.040
2.0	74.563 ± 3.634	72.556 ± 3.819	74.459 ± 3.808	73.940 ± 3.741	67.001 ± 2.997	65.144 ± 2.945	74.918 ± 4.231
3.0	74.742 ± 3.833	72.814 ± 3.668	74.812 ± 3.897	74.913 ± 3.833	69.641 ± 3.490	68.392 ± 3.249	74.473 ± 4.305
4.0	75.017 ± 3.864	72.908 ± 3.733	75.122 ± 3.949	75.216 ± 3.679	72.248 ± 3.682	70.200 ± 3.341	74.227 ± 4.441
5.0	74.980 ± 3.860	72.929 ± 3.729	75.037 ± 3.703	75.338 ± 3.621	73.653 ± 3.646	71.930 ± 3.452	74.101 ± 4.527

Table 8: Results for the Australian Credit Approval dataset.

BR	RF(nt_500)	RF(qs_ent)	RF(mn_4)	RF(mn_8)	RF(ml_4)	RF(ml_5)	RF(nf_all)
0.2	86.946 ± 1.397	86.680 ± 1.431	86.727 ± 1.451	86.634 ± 1.430	86.312 ± 1.469	86.151 ± 1.512	86.208 ± 1.450
0.4	87.151 ± 1.370	86.986 ± 1.429	86.974 ± 1.479	86.810 ± 1.413	86.714 ± 1.419	86.564 ± 1.400	86.525 ± 1.461
0.6	87.225 ± 1.399	87.087 ± 1.415	87.062 ± 1.422	86.945 ± 1.355	86.920 ± 1.407	86.773 ± 1.429	86.541 ± 1.443
0.8	87.199 ± 1.411	87.098 ± 1.436	87.135 ± 1.393	87.067 ± 1.400	86.947 ± 1.409	86.812 ± 1.436	86.404 ± 1.490
1.0	87.214 ± 1.409	87.070 ± 1.430	87.089 ± 1.368	87.062 ± 1.376	86.953 ± 1.409	86.901 ± 1.454	86.130 ± 1.484
1.2	87.188 ± 1.367	87.114 ± 1.363	87.059 ± 1.393	87.055 ± 1.363	86.990 ± 1.430	86.956 ± 1.371	85.850 ± 1.602
2.0	87.051 ± 1.356	87.018 ± 1.413	87.022 ± 1.401	87.025 ± 1.412	87.105 ± 1.459	87.018 ± 1.405	84.980 ± 1.749
3.0	86.989 ± 1.373	86.878 ± 1.381	86.917 ± 1.342	86.999 ± 1.368	87.096 ± 1.366	87.104 ± 1.425	84.350 ± 1.891
4.0	86.944 ± 1.346	86.821 ± 1.385	86.841 ± 1.417	86.888 ± 1.367	87.078 ± 1.373	87.070 ± 1.410	83.967 ± 1.852
5.0	86.911 ± 1.375	86.824 ± 1.366	86.844 ± 1.423	86.891 ± 1.388	87.073 ± 1.413	87.076 ± 1.345	83.723 ± 1.931

Table 9: Results for the Balance Scale dataset.

BR	RF(nt_500)	RF(qs_ent)	RF(mn_4)	RF(mn_8)	RF(ml_4)	RF(ml_5)	RF(nf_all)
0.2	85.972 ± 1.474	85.018 ± 1.595	85.404 ± 1.599	85.519 ± 1.766	85.454 ± 1.914	85.296 ± 2.031	84.374 ± 1.747
0.4	84.732 ± 1.452	84.095 ± 1.441	84.649 ± 1.527	84.895 ± 1.719	85.386 ± 1.800	85.283 ± 1.877	82.641 ± 1.830
0.6	83.947 ± 1.427	83.416 ± 1.440	84.227 ± 1.549	84.487 ± 1.652	84.906 ± 1.668	84.959 ± 1.792	81.262 ± 1.775
0.8	83.329 ± 1.493	82.786 ± 1.435	83.811 ± 1.464	84.268 ± 1.595	84.635 ± 1.705	84.664 ± 1.765	80.093 ± 1.887
1.0	82.831 ± 1.449	82.333 ± 1.582	83.593 ± 1.489	84.180 ± 1.585	84.490 ± 1.682	84.547 ± 1.719	79.090 ± 1.913
1.2	82.483 ± 1.445	81.907 ± 1.519	82.909 ± 1.497	83.936 ± 1.582	84.319 ± 1.667	84.341 ± 1.708	78.248 ± 1.864
2.0	81.581 ± 1.538	81.143 ± 1.593	81.958 ± 1.603	83.419 ± 1.518	83.913 ± 1.538	84.051 ± 1.590	76.734 ± 1.969
3.0	81.256 ± 1.579	80.743 ± 1.629	81.097 ± 1.655	82.447 ± 1.562	83.619 ± 1.497	83.661 ± 1.561	76.189 ± 2.062
4.0	81.029 ± 1.563	80.670 ± 1.628	80.938 ± 1.604	81.811 ± 1.567	83.263 ± 1.442	83.512 ± 1.522	75.956 ± 2.133
5.0	81.015 ± 1.614	80.616 ± 1.625	80.712 ± 1.610	81.326 ± 1.583	82.771 ± 1.516	83.185 ± 1.564	75.788 ± 2.113

Table 10: Results for the Breast Cancer Wisc. (Diag.) dataset.

BR	RF(nt_500)	RF(qs_ent)	RF(mn_4)	RF(mn_8)	RF(ml_4)	RF(ml_5)	RF(nf_all)
0.2	94.673 ± 1.126	94.598 ± 1.201	94.460 ± 1.194	94.289 ± 1.163	93.794 ± 1.273	93.567 ± 1.316	94.367 ± 1.365
0.4	95.076 ± 1.081	95.080 ± 1.171	94.880 ± 1.112	94.664 ± 1.121	94.487 ± 1.222	94.291 ± 1.277	94.704 ± 1.257
0.6	95.257 ± 1.111	95.314 ± 1.163	95.147 ± 1.130	94.924 ± 1.117	94.730 ± 1.144	94.615 ± 1.193	94.876 ± 1.313
0.8	95.360 ± 1.153	95.494 ± 1.144	95.241 ± 1.203	95.061 ± 1.187	94.922 ± 1.164	94.746 ± 1.194	94.942 ± 1.350
1.0	95.459 ± 1.138	95.606 ± 1.171	95.346 ± 1.140	95.122 ± 1.163	94.970 ± 1.146	94.829 ± 1.206	94.930 ± 1.383
1.2	95.540 ± 1.165	95.675 ± 1.168	95.511 ± 1.186	95.309 ± 1.152	95.176 ± 1.188	95.087 ± 1.168	94.822 ± 1.371
2.0	95.651 ± 1.202	95.870 ± 1.110	95.710 ± 1.165	95.600 ± 1.181	95.387 ± 1.183	95.265 ± 1.172	94.536 ± 1.374
3.0	95.724 ± 1.168	95.871 ± 1.113	95.743 ± 1.188	95.642 ± 1.179	95.544 ± 1.167	95.500 ± 1.163	94.256 ± 1.398
4.0	95.692 ± 1.172	95.897 ± 1.108	95.714 ± 1.188	95.699 ± 1.186	95.607 ± 1.156	95.518 ± 1.146	94.154 ± 1.462
5.0	95.691 ± 1.152	95.898 ± 1.095	95.702 ± 1.178	95.704 ± 1.151	95.619 ± 1.166	95.550 ± 1.176	94.007 ± 1.442

Table 11: Results for the Breast Cancer Wisc. (Orig.) dataset.

BR	RF(nt_500)	RF(qs_ent)	RF(mn_4)	RF(mn_8)	RF(ml_4)	RF(ml_5)	RF(nf_all)
0.2	95.366 ± 1.105	95.212 ± 1.144	95.321 ± 1.128	95.454 ± 1.123	95.458 ± 1.128	95.423 ± 1.112	94.517 ± 1.298
0.4	95.506 ± 1.085	95.309 ± 1.113	95.350 ± 1.113	95.474 ± 1.142	95.422 ± 1.160	95.386 ± 1.200	94.552 ± 1.255
0.6	95.491 ± 1.085	95.362 ± 1.127	95.440 ± 1.112	95.501 ± 1.118	95.435 ± 1.138	95.415 ± 1.170	94.570 ± 1.286
0.8	95.457 ± 1.070	95.342 ± 1.135	95.403 ± 1.103	95.440 ± 1.122	95.411 ± 1.124	95.376 ± 1.133	94.521 ± 1.274
1.0	95.429 ± 1.055	95.287 ± 1.087	95.355 ± 1.097	95.433 ± 1.116	95.401 ± 1.099	95.382 ± 1.105	94.407 ± 1.309
1.2	95.378 ± 1.077	95.247 ± 1.081	95.312 ± 1.109	95.394 ± 1.120	95.393 ± 1.130	95.403 ± 1.118	94.336 ± 1.357
2.0	95.262 ± 1.086	95.162 ± 1.109	95.176 ± 1.112	95.233 ± 1.095	95.341 ± 1.111	95.324 ± 1.108	93.919 ± 1.473
3.0	95.166 ± 1.105	95.133 ± 1.110	95.091 ± 1.124	95.151 ± 1.142	95.249 ± 1.138	95.279 ± 1.174	93.516 ± 1.569
4.0	95.155 ± 1.134	95.102 ± 1.124	95.026 ± 1.140	95.089 ± 1.124	95.179 ± 1.132	95.207 ± 1.145	93.316 ± 1.590
5.0	95.115 ± 1.120	95.064 ± 1.128	95.024 ± 1.153	95.047 ± 1.133	95.145 ± 1.104	95.183 ± 1.107	93.100 ± 1.618

Table 12: Results for the Congressional Voting Rec. dataset.

BR	RF(nt_500)	RF(qs_ent)	RF(mn_4)	RF(mn_8)	RF(ml_4)	RF(ml_5)	RF(nf_all)
0.2	93.690 ± 1.487	93.918 ± 1.474	93.819 ± 1.437	93.687 ± 1.439	92.997 ± 1.550	92.795 ± 1.658	94.404 ± 1.337
0.4	94.355 ± 1.520	94.412 ± 1.509	94.278 ± 1.471	93.974 ± 1.410	93.683 ± 1.421	93.534 ± 1.469	94.373 ± 1.394
0.6	94.592 ± 1.480	94.640 ± 1.489	94.509 ± 1.517	94.202 ± 1.429	93.807 ± 1.380	93.747 ± 1.428	94.301 ± 1.448
0.8	94.661 ± 1.494	94.692 ± 1.471	94.637 ± 1.519	94.377 ± 1.483	93.886 ± 1.462	93.800 ± 1.449	94.156 ± 1.453
1.0	94.702 ± 1.431	94.683 ± 1.451	94.686 ± 1.490	94.512 ± 1.500	94.028 ± 1.489	93.890 ± 1.455	93.915 ± 1.579
1.2	94.681 ± 1.457	94.662 ± 1.442	94.763 ± 1.480	94.652 ± 1.504	94.276 ± 1.524	94.099 ± 1.484	93.702 ± 1.684
2.0	94.675 ± 1.426	94.604 ± 1.443	94.753 ± 1.455	94.795 ± 1.474	94.481 ± 1.540	94.317 ± 1.505	93.139 ± 1.782
3.0	94.620 ± 1.413	94.569 ± 1.389	94.605 ± 1.457	94.760 ± 1.461	94.705 ± 1.485	94.620 ± 1.515	92.788 ± 1.878
4.0	94.615 ± 1.413	94.539 ± 1.423	94.575 ± 1.394	94.703 ± 1.433	94.756 ± 1.501	94.722 ± 1.513	92.721 ± 1.931
5.0	94.621 ± 1.432	94.520 ± 1.451	94.520 ± 1.404	94.633 ± 1.425	94.791 ± 1.472	94.769 ± 1.483	92.645 ± 1.922

Table 13: Results for the Echocardiogram dataset.

BR	RF(nt_500)	RF(qs_ent)	RF(mn_4)	RF(mn_8)	RF(ml_4)	RF(ml_5)	RF(nf_all)
0.2	70.774 ± 2.633	70.992 ± 2.462	71.153 ± 2.174	70.968 ± 0.000	70.968 ± 0.000	70.968 ± 0.000	71.226 ± 3.311
0.4	71.242 ± 4.116	71.435 ± 3.788	71.524 ± 3.908	71.427 ± 3.500	70.944 ± 0.665	70.968 ± 0.000	71.718 ± 4.577
0.6	72.024 ± 4.493	72.468 ± 4.497	72.500 ± 4.746	72.315 ± 4.755	71.766 ± 3.347	71.056 ± 2.374	72.000 ± 5.264
0.8	71.790 ± 5.039	72.258 ± 5.018	72.524 ± 4.697	72.581 ± 4.823	72.444 ± 3.855	71.944 ± 3.446	70.774 ± 6.117
1.0	71.831 ± 4.925	72.298 ± 5.077	72.306 ± 5.037	72.685 ± 4.923	72.645 ± 4.224	72.403 ± 3.853	70.500 ± 6.162
1.2	71.766 ± 5.117	72.008 ± 5.478	72.008 ± 5.353	72.718 ± 5.119	73.048 ± 4.601	72.976 ± 4.423	69.919 ± 6.735
2.0	71.589 ± 5.629	71.581 ± 6.115	71.565 ± 5.413	72.331 ± 5.516	72.887 ± 5.019	73.113 ± 5.005	68.355 ± 7.291
3.0	71.387 ± 5.876	71.927 ± 6.038	71.266 ± 5.837	72.194 ± 5.717	72.935 ± 5.458	73.065 ± 5.224	68.105 ± 7.742
4.0	71.419 ± 6.142	71.460 ± 5.895	71.177 ± 5.918	71.403 ± 5.795	72.540 ± 5.775	72.815 ± 5.564	67.847 ± 7.604
5.0	71.234 ± 6.367	71.734 ± 6.113	71.161 ± 6.173	71.387 ± 5.916	72.234 ± 5.867	72.452 ± 5.595	67.419 ± 8.158

Table 14: Results for the Ecoli dataset.

BR	RF(nt_500)	RF(qs_ent)	RF(mn_4)	RF(mn_8)	RF(ml_4)	RF(ml_5)	RF(nf_all)
0.2	84.060 ± 1.965	83.714 ± 2.027	83.295 ± 2.017	79.817 ± 2.070	76.765 ± 1.462	76.155 ± 1.311	84.161 ± 1.945
0.4	85.527 ± 1.799	84.943 ± 1.886	85.220 ± 1.942	84.589 ± 1.864	81.098 ± 1.966	78.716 ± 1.762	84.644 ± 1.994
0.6	85.835 ± 1.858	85.263 ± 1.928	85.680 ± 1.843	85.378 ± 1.922	83.496 ± 1.856	82.314 ± 1.962	84.339 ± 2.127
0.8	85.671 ± 1.872	85.164 ± 1.926	85.580 ± 2.000	85.452 ± 1.914	84.201 ± 1.834	83.573 ± 1.996	83.664 ± 2.242
1.0	85.565 ± 1.905	85.082 ± 1.949	85.589 ± 1.975	85.509 ± 1.924	84.560 ± 1.868	84.170 ± 1.912	83.049 ± 2.438
1.2	85.321 ± 1.981	84.933 ± 1.996	85.592 ± 1.928	85.554 ± 1.939	85.046 ± 1.895	84.647 ± 1.905	82.658 ± 2.535
2.0	84.859 ± 2.041	84.394 ± 2.073	85.006 ± 2.060	85.351 ± 2.069	85.106 ± 1.968	84.902 ± 1.945	81.269 ± 2.666
3.0	84.604 ± 2.054	84.104 ± 2.132	84.621 ± 2.049	84.946 ± 2.020	85.171 ± 2.015	85.070 ± 1.976	80.528 ± 2.765
4.0	84.490 ± 2.110	83.978 ± 2.036	84.439 ± 2.111	84.690 ± 2.096	85.019 ± 2.050	85.054 ± 1.999	80.137 ± 2.788
5.0	84.369 ± 2.111	83.912 ± 2.060	84.348 ± 2.103	84.568 ± 2.130	84.876 ± 2.011	84.990 ± 2.051	79.839 ± 2.765

Table 15: Results for the German Credit Data dataset.

BR	RF(nt_500)	RF(qs_ent)	RF(mn_4)	RF(mn_8)	RF(ml_4)	RF(ml_5)	RF(nf_all)
0.2	73.932 ± 1.059	73.797 ± 1.169	73.614 ± 1.169	73.195 ± 1.066	71.769 ± 0.839	71.227 ± 0.738	74.612 ± 1.322
0.4	75.023 ± 1.137	74.778 ± 1.190	74.700 ± 1.159	74.337 ± 1.176	73.230 ± 1.031	72.766 ± 0.938	75.046 ± 1.416
0.6	75.312 ± 1.110	75.072 ± 1.172	74.996 ± 1.262	74.816 ± 1.201	73.879 ± 1.090	73.483 ± 1.084	74.919 ± 1.423
0.8	75.410 ± 1.149	75.157 ± 1.199	75.127 ± 1.222	74.954 ± 1.223	74.276 ± 1.137	73.908 ± 1.113	74.567 ± 1.524
1.0	75.397 ± 1.150	75.195 ± 1.232	75.170 ± 1.197	75.174 ± 1.190	74.510 ± 1.164	74.178 ± 1.175	74.344 ± 1.615
1.2	75.466 ± 1.196	75.296 ± 1.272	75.262 ± 1.240	75.153 ± 1.242	74.798 ± 1.168	74.636 ± 1.164	74.127 ± 1.597
2.0	75.352 ± 1.196	75.113 ± 1.263	75.164 ± 1.280	75.154 ± 1.209	75.114 ± 1.217	75.035 ± 1.226	73.342 ± 1.655
3.0	75.375 ± 1.211	75.078 ± 1.209	75.082 ± 1.299	75.164 ± 1.303	75.324 ± 1.197	75.207 ± 1.191	72.835 ± 1.749
4.0	75.349 ± 1.226	75.073 ± 1.302	75.007 ± 1.288	75.124 ± 1.263	75.252 ± 1.256	75.249 ± 1.225	72.440 ± 1.781
5.0	75.322 ± 1.218	75.106 ± 1.280	75.110 ± 1.244	75.178 ± 1.279	75.216 ± 1.278	75.245 ± 1.348	72.175 ± 1.742

Table 16: Results for the Glass Identification dataset.

BR	RF(nt_500)	RF(qs_ent)	RF(mn_4)	RF(mn_8)	RF(ml_4)	RF(ml_5)	RF(nf_all)
0.2	67.159 ± 3.839	67.054 ± 3.664	65.267 ± 3.704	63.493 ± 3.843	61.211 ± 3.696	60.005 ± 3.950	65.789 ± 3.919
0.4	72.204 ± 3.639	72.366 ± 3.629	70.746 ± 3.679	67.456 ± 3.605	65.249 ± 3.781	64.087 ± 3.939	71.043 ± 3.915
0.6	74.004 ± 3.690	74.222 ± 3.719	72.821 ± 3.492	70.084 ± 3.738	67.529 ± 3.871	66.000 ± 3.737	72.572 ± 3.927
0.8	74.934 ± 3.675	74.812 ± 3.579	73.941 ± 3.784	71.793 ± 3.779	69.305 ± 3.829	67.435 ± 3.690	72.891 ± 3.877
1.0	75.250 ± 3.652	75.154 ± 3.608	74.346 ± 3.865	72.728 ± 3.859	70.676 ± 3.851	68.794 ± 3.761	72.829 ± 3.958
1.2	75.413 ± 3.695	75.424 ± 3.659	74.727 ± 3.768	73.748 ± 3.932	72.845 ± 3.870	71.479 ± 3.804	72.798 ± 3.983
2.0	75.577 ± 3.698	75.596 ± 3.778	75.176 ± 3.813	74.460 ± 3.889	74.366 ± 3.795	73.659 ± 3.823	71.466 ± 4.357
3.0	75.429 ± 3.751	75.383 ± 3.969	74.927 ± 3.667	74.819 ± 3.593	74.840 ± 3.687	74.624 ± 3.789	70.340 ± 4.430
4.0	75.328 ± 3.788	75.457 ± 3.842	74.848 ± 3.641	74.708 ± 3.744	74.868 ± 3.641	74.725 ± 3.698	69.839 ± 4.622
5.0	75.295 ± 3.721	75.363 ± 3.920	74.923 ± 3.736	74.838 ± 3.877	75.037 ± 3.738	74.931 ± 3.725	69.432 ± 4.705

Table 17: Results for the Heart dataset.

BR	RF(nt_500)	RF(qs_ent)	RF(mn_4)	RF(mn_8)	RF(ml_4)	RF(ml_5)	RF(nf_all)
0.2	83.319 ± 2.532	82.794 ± 2.558	82.969 ± 2.641	82.924 ± 2.685	83.324 ± 2.569	83.217 ± 2.502	81.669 ± 2.773
0.4	82.693 ± 2.339	82.406 ± 2.480	82.696 ± 2.461	82.806 ± 2.542	83.294 ± 2.553	83.224 ± 2.662	81.289 ± 2.810
0.6	82.272 ± 2.432	82.019 ± 2.495	82.243 ± 2.514	82.472 ± 2.505	83.137 ± 2.650	83.119 ± 2.584	80.676 ± 2.961
0.8	81.907 ± 2.465	81.800 ± 2.614	82.061 ± 2.490	82.352 ± 2.558	82.981 ± 2.534	83.148 ± 2.617	80.409 ± 2.981
1.0	81.689 ± 2.472	81.639 ± 2.565	81.846 ± 2.545	82.272 ± 2.470	82.933 ± 2.555	82.993 ± 2.525	79.961 ± 3.096
1.2	81.506 ± 2.501	81.372 ± 2.551	81.578 ± 2.623	81.917 ± 2.569	82.594 ± 2.550	82.830 ± 2.556	79.502 ± 2.959
2.0	81.046 ± 2.466	80.894 ± 2.481	80.946 ± 2.510	81.361 ± 2.428	82.093 ± 2.390	82.435 ± 2.453	78.394 ± 3.078
3.0	80.854 ± 2.523	80.707 ± 2.517	80.744 ± 2.465	81.083 ± 2.619	81.750 ± 2.612	81.989 ± 2.632	77.691 ± 3.164
4.0	80.813 ± 2.517	80.639 ± 2.563	80.680 ± 2.578	80.926 ± 2.610	81.441 ± 2.609	81.539 ± 2.475	77.250 ± 3.278
5.0	80.774 ± 2.541	80.691 ± 2.510	80.583 ± 2.552	80.835 ± 2.582	81.180 ± 2.652	81.322 ± 2.607	77.019 ± 3.233

Table 18: Results for the Hepatitis dataset.

BR	RF(nt_500)	RF(qs_ent)	RF(mn_4)	RF(mn_8)	RF(ml_4)	RF(ml_5)	RF(nf_all)
0.2	83.399 ± 2.143	82.936 ± 2.195	82.858 ± 2.107	82.081 ± 1.879	79.730 ± 0.000	79.730 ± 0.000	84.115 ± 2.303
0.4	84.726 ± 2.600	84.287 ± 2.784	84.149 ± 2.513	83.760 ± 2.454	80.831 ± 1.246	79.943 ± 0.501	84.044 ± 3.243
0.6	84.561 ± 2.587	84.446 ± 2.868	84.220 ± 2.789	84.189 ± 2.575	82.530 ± 1.869	81.128 ± 1.384	83.645 ± 3.406
0.8	84.355 ± 2.823	84.243 ± 2.997	84.270 ± 2.976	84.226 ± 2.794	83.439 ± 2.194	82.537 ± 1.866	83.233 ± 3.526
1.0	84.318 ± 2.889	84.216 ± 3.067	83.993 ± 3.007	84.176 ± 2.886	83.838 ± 2.281	83.236 ± 2.111	82.720 ± 3.387
1.2	84.341 ± 2.899	84.274 ± 2.999	83.993 ± 3.004	84.108 ± 2.986	84.206 ± 2.530	83.905 ± 2.335	82.274 ± 3.660
2.0	84.111 ± 3.048	84.095 ± 3.154	84.020 ± 3.136	83.970 ± 3.050	84.166 ± 2.772	84.169 ± 2.627	81.081 ± 3.963
3.0	84.020 ± 3.081	84.061 ± 3.223	83.760 ± 3.168	83.905 ± 3.138	84.020 ± 2.928	84.068 ± 2.862	80.436 ± 4.001
4.0	83.976 ± 3.042	83.895 ± 3.169	83.723 ± 3.068	83.851 ± 3.163	84.027 ± 2.988	83.983 ± 2.959	80.068 ± 4.158
5.0	83.983 ± 3.152	83.922 ± 3.131	83.672 ± 3.239	83.696 ± 3.054	83.814 ± 3.100	83.929 ± 2.956	79.959 ± 4.031

Table 19: Results for the Horse Colic dataset.

BR	RF(nt_500)	RF(qs_ent)	RF(mn_4)	RF(mn_8)	RF(ml_4)	RF(ml_5)	RF(nf_all)
0.2	85.883 ± 1.902	85.681 ± 1.959	85.645 ± 1.848	85.685 ± 1.904	84.041 ± 2.054	82.474 ± 2.331	84.861 ± 2.541
0.4	86.111 ± 1.882	85.933 ± 1.905	86.056 ± 1.812	86.090 ± 1.837	85.670 ± 1.840	85.458 ± 1.822	86.052 ± 2.245
0.6	86.285 ± 1.872	86.240 ± 1.858	86.193 ± 1.855	86.230 ± 1.843	85.780 ± 1.860	85.698 ± 1.878	86.269 ± 2.141
0.8	86.484 ± 1.879	86.279 ± 1.903	86.315 ± 1.932	86.216 ± 1.881	85.815 ± 1.907	85.774 ± 1.798	86.095 ± 2.068
1.0	86.516 ± 1.918	86.311 ± 1.852	86.303 ± 1.808	86.197 ± 1.805	85.818 ± 1.927	85.766 ± 1.826	85.769 ± 2.199
1.2	86.515 ± 1.888	86.365 ± 1.855	86.371 ± 1.910	86.295 ± 1.827	85.856 ± 1.839	85.780 ± 1.875	85.387 ± 2.231
2.0	86.438 ± 1.871	86.226 ± 1.920	86.360 ± 1.873	86.383 ± 1.901	85.887 ± 1.998	85.781 ± 1.962	84.645 ± 2.301
3.0	86.480 ± 1.872	86.202 ± 1.919	86.306 ± 1.886	86.421 ± 1.902	86.144 ± 1.953	85.950 ± 1.870	84.007 ± 2.395
4.0	86.395 ± 1.844	86.148 ± 1.928	86.156 ± 1.915	86.205 ± 1.865	86.167 ± 1.926	86.163 ± 1.899	83.776 ± 2.420
5.0	86.414 ± 1.846	86.177 ± 1.797	86.261 ± 1.926	86.276 ± 1.861	86.216 ± 1.936	86.166 ± 1.941	83.569 ± 2.373

Table 20: Results for the Image Segmentation (Stat.) dataset.

BR	RF(nt_500)	RF(qs_ent)	RF(mn_4)	RF(mn_8)	RF(ml_4)	RF(ml_5)	RF(nf_all)
0.2	95.150 ± 0.754	95.081 ± 0.718	94.914 ± 0.783	94.360 ± 0.816	93.540 ± 0.785	93.179 ± 0.774	95.126 ± 0.739
0.4	96.213 ± 0.583	96.143 ± 0.605	96.049 ± 0.615	95.634 ± 0.679	94.868 ± 0.759	94.518 ± 0.798	95.859 ± 0.662
0.6	96.511 ± 0.539	96.502 ± 0.577	96.418 ± 0.555	96.130 ± 0.581	95.465 ± 0.681	95.151 ± 0.722	96.070 ± 0.612
0.8	96.712 ± 0.528	96.718 ± 0.559	96.608 ± 0.548	96.365 ± 0.547	95.802 ± 0.645	95.519 ± 0.665	96.150 ± 0.621
1.0	96.825 ± 0.509	96.843 ± 0.563	96.728 ± 0.544	96.498 ± 0.564	95.996 ± 0.625	95.720 ± 0.663	96.184 ± 0.631
1.2	96.898 ± 0.513	96.924 ± 0.522	96.814 ± 0.528	96.680 ± 0.549	96.328 ± 0.589	96.104 ± 0.618	96.190 ± 0.625
2.0	97.018 ± 0.512	97.071 ± 0.539	96.967 ± 0.524	96.876 ± 0.529	96.604 ± 0.552	96.479 ± 0.548	96.094 ± 0.662
3.0	97.064 ± 0.525	97.107 ± 0.522	96.989 ± 0.532	96.993 ± 0.524	96.805 ± 0.548	96.702 ± 0.553	95.970 ± 0.669
4.0	97.081 ± 0.521	97.130 ± 0.544	97.023 ± 0.523	97.017 ± 0.537	96.906 ± 0.539	96.824 ± 0.525	95.842 ± 0.690
5.0	97.080 ± 0.530	97.133 ± 0.538	97.018 ± 0.538	97.013 ± 0.544	96.939 ± 0.540	96.880 ± 0.554	95.773 ± 0.692

Table 21: Results for the Ionosphere dataset.

BR	RF(nt_500)	RF(qs_ent)	RF(mn_4)	RF(mn_8)	RF(ml_4)	RF(ml_5)	RF(nf_all)
0.2	92.629 ± 1.511	91.544 ± 1.839	91.913 ± 1.651	91.934 ± 1.701	88.669 ± 2.406	86.764 ± 2.230	91.700 ± 1.979
0.4	93.076 ± 1.448	92.580 ± 1.591	92.643 ± 1.533	92.511 ± 1.575	91.760 ± 1.758	91.183 ± 1.996	92.256 ± 2.013
0.6	93.194 ± 1.495	92.753 ± 1.513	92.699 ± 1.550	92.666 ± 1.538	92.253 ± 1.611	91.986 ± 1.685	92.190 ± 2.083
0.8	93.209 ± 1.475	92.937 ± 1.544	92.829 ± 1.547	92.707 ± 1.561	92.443 ± 1.574	92.310 ± 1.635	91.961 ± 2.139
1.0	93.231 ± 1.524	93.024 ± 1.499	92.881 ± 1.493	92.764 ± 1.564	92.591 ± 1.587	92.400 ± 1.593	91.730 ± 2.169
1.2	93.254 ± 1.526	93.020 ± 1.588	92.903 ± 1.637	92.814 ± 1.613	92.776 ± 1.586	92.630 ± 1.593	91.571 ± 2.190
2.0	93.233 ± 1.595	93.070 ± 1.556	92.957 ± 1.640	92.851 ± 1.627	92.843 ± 1.572	92.770 ± 1.592	90.896 ± 2.281
3.0	93.229 ± 1.600	93.099 ± 1.608	93.003 ± 1.614	92.906 ± 1.615	92.897 ± 1.594	92.836 ± 1.572	90.474 ± 2.443
4.0	93.240 ± 1.598	93.103 ± 1.523	93.010 ± 1.632	92.956 ± 1.709	92.844 ± 1.627	92.881 ± 1.597	90.151 ± 2.442
5.0	93.237 ± 1.571	93.127 ± 1.577	93.039 ± 1.615	92.964 ± 1.625	92.911 ± 1.604	92.927 ± 1.559	89.920 ± 2.498

Table 22: Results for the Iris dataset.

BR	RF(nt_500)	RF(qs_ent)	RF(mn_4)	RF(mn_8)	RF(ml_4)	RF(ml_5)	RF(nf_all)
0.2	95.178 ± 1.824	95.098 ± 1.833	95.171 ± 1.876	95.199 ± 1.899	95.095 ± 1.951	94.880 ± 2.076	95.218 ± 1.840
0.4	95.115 ± 1.831	95.058 ± 1.804	95.232 ± 1.900	95.185 ± 1.878	95.155 ± 1.835	95.212 ± 1.860	95.084 ± 1.856
0.6	95.010 ± 1.870	94.947 ± 1.863	95.145 ± 1.941	95.185 ± 1.983	95.081 ± 1.923	95.081 ± 1.949	95.017 ± 1.901
0.8	94.967 ± 1.892	94.859 ± 1.883	95.091 ± 1.982	95.131 ± 2.049	94.963 ± 1.986	94.947 ± 1.980	94.940 ± 1.926
1.0	94.950 ± 1.904	94.863 ± 1.915	95.064 ± 1.972	95.101 ± 2.033	94.920 ± 2.030	94.859 ± 1.989	94.886 ± 1.947
1.2	94.917 ± 1.890	94.860 ± 1.931	95.020 ± 1.977	95.138 ± 2.050	94.919 ± 2.036	94.896 ± 2.015	94.883 ± 1.989
2.0	94.863 ± 1.919	94.826 ± 1.915	94.933 ± 1.942	95.155 ± 2.053	94.943 ± 2.067	94.876 ± 2.039	94.624 ± 2.239
3.0	94.883 ± 1.893	94.819 ± 1.865	94.842 ± 1.929	95.054 ± 1.989	94.947 ± 2.000	95.001 ± 2.102	94.517 ± 2.294
4.0	94.839 ± 1.898	94.816 ± 1.928	94.812 ± 1.916	94.964 ± 1.959	94.897 ± 1.976	94.954 ± 2.050	94.517 ± 2.223
5.0	94.849 ± 1.914	94.806 ± 1.895	94.792 ± 1.899	94.890 ± 1.955	94.833 ± 1.946	94.897 ± 1.981	94.500 ± 2.237

Table 23: Results for the Labor Relations dataset.

BR	RF(nt_500)	RF(qs_ent)	RF(mn_4)	RF(mn_8)	RF(ml_4)	RF(ml_5)	RF(nf_all)
0.2	82.500 ± 5.787	83.768 ± 6.384	80.735 ± 6.456	64.901 ± 0.616	64.901 ± 0.616	64.901 ± 0.616	84.817 ± 6.153
0.4	90.273 ± 5.306	90.113 ± 5.135	89.246 ± 5.120	84.780 ± 5.871	66.436 ± 2.657	64.901 ± 0.616	88.058 ± 5.846
0.6	92.629 ± 4.660	92.268 ± 4.704	91.790 ± 4.777	90.437 ± 4.619	78.279 ± 5.683	70.293 ± 4.840	89.736 ± 5.886
0.8	93.227 ± 4.407	92.929 ± 4.537	92.682 ± 4.575	91.825 ± 4.584	83.577 ± 5.449	77.870 ± 5.680	90.354 ± 5.748
1.0	93.381 ± 4.478	92.865 ± 4.579	92.837 ± 4.656	92.354 ± 4.416	85.311 ± 5.239	80.514 ± 5.594	90.369 ± 5.799
1.2	93.608 ± 4.329	93.374 ± 4.445	93.339 ± 4.390	92.699 ± 4.447	89.673 ± 4.926	87.363 ± 5.051	89.845 ± 6.026
2.0	93.522 ± 4.419	93.408 ± 4.362	93.346 ± 4.447	93.222 ± 4.362	91.798 ± 4.772	90.671 ± 4.840	88.915 ± 6.119
3.0	93.445 ± 4.414	93.332 ± 4.374	93.191 ± 4.356	93.127 ± 4.388	92.531 ± 4.538	92.169 ± 4.463	88.321 ± 6.562
4.0	93.496 ± 4.366	93.365 ± 4.392	93.375 ± 4.313	93.215 ± 4.309	93.065 ± 4.282	92.723 ± 4.303	87.866 ± 6.702
5.0	93.462 ± 4.390	93.304 ± 4.448	93.127 ± 4.415	93.111 ± 4.468	93.077 ± 4.445	92.750 ± 4.578	87.597 ± 6.552

Table 24: Results for the Liver Disorders dataset.

BR	RF(nt_500)	RF(qs_ent)	RF(mn_4)	RF(mn_8)	RF(ml_4)	RF(ml_5)	RF(nf_all)
0.2	59.507 ± 2.770	59.089 ± 2.991	59.164 ± 2.827	59.485 ± 3.014	59.714 ± 2.951	59.711 ± 2.870	59.213 ± 2.791
0.4	58.570 ± 2.799	58.240 ± 2.868	58.406 ± 2.697	58.757 ± 2.760	59.109 ± 2.816	59.209 ± 2.880	58.219 ± 2.778
0.6	57.910 ± 2.817	57.616 ± 2.845	57.923 ± 3.027	58.482 ± 2.786	58.921 ± 2.846	59.206 ± 2.851	57.605 ± 2.928
0.8	57.391 ± 2.867	57.352 ± 2.883	57.752 ± 2.896	58.259 ± 2.828	58.825 ± 2.831	59.186 ± 2.841	56.903 ± 2.998
1.0	57.016 ± 2.746	57.061 ± 3.103	57.387 ± 2.934	57.916 ± 2.934	58.635 ± 2.860	58.991 ± 2.877	56.614 ± 2.884
1.2	56.752 ± 2.880	56.638 ± 2.901	56.961 ± 2.938	57.399 ± 2.883	58.183 ± 2.858	58.446 ± 2.739	56.409 ± 3.139
2.0	56.160 ± 2.936	55.975 ± 3.188	56.290 ± 3.053	56.956 ± 2.935	57.720 ± 2.865	57.935 ± 2.867	55.569 ± 3.149
3.0	55.751 ± 3.008	55.612 ± 3.181	55.826 ± 3.100	56.144 ± 3.027	56.830 ± 2.886	57.326 ± 3.121	55.075 ± 3.227
4.0	55.755 ± 3.067	55.578 ± 3.134	55.721 ± 3.039	55.867 ± 3.113	56.548 ± 3.034	56.877 ± 3.091	54.922 ± 3.159
5.0	55.645 ± 3.090	55.452 ± 3.043	55.755 ± 3.006	55.776 ± 3.166	56.301 ± 3.055	56.460 ± 2.977	54.812 ± 3.189

Table 25: Results for the Optical Recognition (Digits) dataset.

BR	RF(nt_500)	RF(qs_ent)	RF(mn_4)	RF(mn_8)	RF(ml_4)	RF(ml_5)	RF(nf_all)
0.2	95.549 ± 0.677	95.168 ± 0.742	94.761 ± 0.739	94.161 ± 0.814	93.207 ± 0.878	92.702 ± 0.884	93.174 ± 0.985
0.4	96.386 ± 0.593	96.156 ± 0.642	95.861 ± 0.679	95.341 ± 0.759	94.507 ± 0.799	94.029 ± 0.788	93.866 ± 0.975
0.6	96.744 ± 0.572	96.553 ± 0.617	96.310 ± 0.623	95.873 ± 0.664	95.094 ± 0.740	94.691 ± 0.747	94.074 ± 0.977
0.8	96.964 ± 0.562	96.811 ± 0.544	96.581 ± 0.571	96.188 ± 0.627	95.488 ± 0.713	95.104 ± 0.759	94.094 ± 1.018
1.0	97.108 ± 0.548	96.933 ± 0.539	96.741 ± 0.580	96.378 ± 0.633	95.717 ± 0.713	95.387 ± 0.711	94.014 ± 1.045
1.2	97.176 ± 0.535	96.986 ± 0.512	96.883 ± 0.572	96.624 ± 0.598	96.108 ± 0.634	95.849 ± 0.684	93.943 ± 1.061
2.0	97.340 ± 0.524	97.194 ± 0.499	97.085 ± 0.564	96.898 ± 0.584	96.536 ± 0.598	96.267 ± 0.642	93.335 ± 1.209
3.0	97.396 ± 0.505	97.246 ± 0.531	97.208 ± 0.527	97.096 ± 0.555	96.794 ± 0.596	96.654 ± 0.601	92.561 ± 1.423
4.0	97.413 ± 0.519	97.255 ± 0.514	97.218 ± 0.540	97.153 ± 0.556	96.977 ± 0.591	96.858 ± 0.599	91.948 ± 1.544
5.0	97.401 ± 0.514	97.263 ± 0.511	97.233 ± 0.539	97.192 ± 0.530	97.050 ± 0.541	96.944 ± 0.581	91.474 ± 1.645

Table 26: Results for the Parkinsons dataset.

BR	RF(nt_500)	RF(qs_ent)	RF(mn_4)	RF(mn_8)	RF(ml_4)	RF(ml_5)	RF(nf_all)
0.2	84.367 ± 3.323	84.487 ± 3.351	83.902 ± 3.371	82.746 ± 3.191	81.979 ± 3.268	81.174 ± 3.147	84.482 ± 3.362
0.4	86.205 ± 3.474	86.203 ± 3.337	85.618 ± 3.554	84.339 ± 3.385	84.187 ± 3.226	83.464 ± 3.141	85.950 ± 3.506
0.6	87.223 ± 3.458	87.413 ± 3.426	86.705 ± 3.585	85.462 ± 3.544	84.993 ± 3.256	84.446 ± 3.294	86.554 ± 3.622
0.8	87.949 ± 3.369	88.085 ± 3.256	87.408 ± 3.375	86.336 ± 3.557	85.757 ± 3.364	85.097 ± 3.383	86.828 ± 3.765
1.0	88.297 ± 3.317	88.354 ± 3.123	87.874 ± 3.369	86.674 ± 3.516	86.275 ± 3.346	85.687 ± 3.400	87.151 ± 3.840
1.2	88.536 ± 3.299	88.736 ± 3.191	88.426 ± 3.260	87.629 ± 3.330	87.069 ± 3.297	86.528 ± 3.318	87.195 ± 3.914
2.0	89.093 ± 3.270	89.150 ± 3.270	88.854 ± 3.136	88.462 ± 3.320	87.782 ± 3.336	87.418 ± 3.404	87.335 ± 4.205
3.0	89.213 ± 3.262	89.244 ± 3.162	89.139 ± 3.216	88.877 ± 3.245	88.482 ± 3.285	88.215 ± 3.268	87.167 ± 4.156
4.0	89.306 ± 3.254	89.206 ± 3.208	89.154 ± 3.123	89.031 ± 3.269	88.628 ± 3.298	88.508 ± 3.275	87.000 ± 4.281
5.0	89.306 ± 3.234	89.160 ± 3.296	89.213 ± 3.070	89.133 ± 3.130	88.810 ± 3.169	88.710 ± 3.194	86.941 ± 4.166

Table 27: Results for the Pima Indians Diabetes dataset.

BR	RF(nt_500)	RF(qs_ent)	RF(mn_4)	RF(mn_8)	RF(ml_4)	RF(ml_5)	RF(nf_all)
0.2	76.344 ± 1.557	75.767 ± 1.632	76.092 ± 1.559	76.144 ± 1.580	75.973 ± 1.505	75.805 ± 1.522	76.333 ± 1.659
0.4	76.285 ± 1.662	76.020 ± 1.555	76.152 ± 1.575	76.086 ± 1.588	76.061 ± 1.561	76.040 ± 1.543	75.995 ± 1.631
0.6	76.161 ± 1.619	76.022 ± 1.647	76.069 ± 1.552	76.099 ± 1.592	76.101 ± 1.578	75.965 ± 1.555	75.912 ± 1.636
0.8	76.071 ± 1.633	75.937 ± 1.609	75.998 ± 1.596	76.100 ± 1.711	76.058 ± 1.620	76.048 ± 1.564	75.566 ± 1.743
1.0	75.950 ± 1.658	75.752 ± 1.627	75.921 ± 1.681	75.984 ± 1.690	76.061 ± 1.636	76.148 ± 1.607	75.316 ± 1.707
1.2	75.883 ± 1.626	75.745 ± 1.648	75.764 ± 1.705	75.999 ± 1.667	76.096 ± 1.649	76.075 ± 1.616	75.107 ± 1.727
2.0	75.736 ± 1.648	75.579 ± 1.617	75.549 ± 1.693	75.736 ± 1.733	75.937 ± 1.637	75.987 ± 1.660	74.475 ± 1.832
3.0	75.500 ± 1.642	75.386 ± 1.675	75.349 ± 1.728	75.578 ± 1.731	75.821 ± 1.641	75.811 ± 1.680	74.051 ± 1.878
4.0	75.517 ± 1.684	75.370 ± 1.714	75.281 ± 1.667	75.446 ± 1.720	75.598 ± 1.613	75.739 ± 1.636	73.600 ± 1.846
5.0	75.449 ± 1.700	75.231 ± 1.705	75.320 ± 1.663	75.378 ± 1.669	75.575 ± 1.635	75.602 ± 1.705	73.443 ± 1.910

Table 28: Results for the Sonar, Mines vs. Rocks dataset.

BR	RF(nt_500)	RF(qs_ent)	RF(mn_4)	RF(mn_8)	RF(ml_4)	RF(ml_5)	RF(nf_all)
0.2	77.678 ± 3.731	76.805 ± 3.706	76.656 ± 3.867	76.327 ± 3.705	76.135 ± 3.647	75.899 ± 3.627	75.820 ± 3.805
0.4	78.594 ± 3.922	78.212 ± 3.900	77.959 ± 3.892	77.404 ± 3.868	77.752 ± 3.845	77.351 ± 3.948	76.356 ± 3.951
0.6	79.120 ± 3.966	79.353 ± 4.033	78.697 ± 4.141	78.159 ± 3.992	78.433 ± 4.140	78.099 ± 4.079	76.887 ± 4.058
0.8	79.572 ± 3.961	79.870 ± 3.937	79.209 ± 4.078	78.442 ± 4.099	78.623 ± 4.087	78.418 ± 4.111	76.803 ± 4.042
1.0	80.214 ± 3.992	80.240 ± 3.903	79.625 ± 4.093	78.894 ± 4.004	79.130 ± 4.014	78.808 ± 4.019	76.897 ± 4.227
1.2	80.618 ± 4.143	80.053 ± 3.981	79.750 ± 4.055	79.296 ± 4.040	79.397 ± 4.041	79.055 ± 3.962	76.894 ± 4.261
2.0	81.236 ± 4.060	81.094 ± 3.975	80.579 ± 4.141	80.276 ± 4.192	80.091 ± 4.045	79.817 ± 4.206	76.548 ± 4.440
3.0	81.486 ± 4.057	81.308 ± 4.024	80.974 ± 3.884	80.656 ± 3.927	80.514 ± 4.021	80.341 ± 4.103	75.822 ± 4.701
4.0	81.565 ± 4.072	81.627 ± 4.007	81.317 ± 4.061	81.113 ± 4.037	80.962 ± 3.934	80.668 ± 3.834	75.464 ± 4.878
5.0	81.548 ± 4.161	81.538 ± 3.989	81.012 ± 4.123	81.161 ± 3.924	80.930 ± 3.939	80.913 ± 4.007	74.950 ± 4.863

Table 29: Results for the Soybean (Large) dataset.

BR	RF(nt_500)	RF(qs_ent)	RF(mn_4)	RF(mn_8)	RF(ml_4)	RF(ml_5)	RF(nf_all)
0.2	90.450 ± 1.379	89.572 ± 1.557	89.425 ± 1.555	86.323 ± 1.798	74.294 ± 2.680	67.276 ± 2.540	89.222 ± 1.595
0.4	91.692 ± 1.346	91.319 ± 1.321	91.410 ± 1.349	90.479 ± 1.479	85.207 ± 1.979	82.423 ± 2.141	91.089 ± 1.541
0.6	92.186 ± 1.312	91.806 ± 1.382	92.050 ± 1.336	91.511 ± 1.395	87.737 ± 1.699	85.760 ± 1.888	91.463 ± 1.516
0.8	92.386 ± 1.280	92.013 ± 1.288	92.268 ± 1.291	91.938 ± 1.319	88.928 ± 1.636	87.261 ± 1.727	91.628 ± 1.467
1.0	92.442 ± 1.282	92.101 ± 1.308	92.459 ± 1.327	92.204 ± 1.316	89.641 ± 1.588	88.136 ± 1.732	91.664 ± 1.474
1.2	92.521 ± 1.296	92.233 ± 1.293	92.440 ± 1.294	92.479 ± 1.278	90.923 ± 1.434	90.044 ± 1.516	91.635 ± 1.488
2.0	92.606 ± 1.299	92.348 ± 1.254	92.598 ± 1.304	92.695 ± 1.263	91.704 ± 1.355	91.182 ± 1.450	91.505 ± 1.509
3.0	92.641 ± 1.300	92.412 ± 1.296	92.618 ± 1.292	92.691 ± 1.240	92.153 ± 1.340	91.985 ± 1.351	91.274 ± 1.564
4.0	92.640 ± 1.251	92.480 ± 1.278	92.561 ± 1.297	92.712 ± 1.276	92.403 ± 1.278	92.220 ± 1.327	91.133 ± 1.613
5.0	92.662 ± 1.246	92.537 ± 1.288	92.566 ± 1.290	92.681 ± 1.314	92.526 ± 1.291	92.387 ± 1.289	91.027 ± 1.623

Table 30: Results for the Tic-Tac-Toe Endgame dataset.

BR	RF(nt_500)	RF(qs_ent)	RF(mn_4)	RF(mn_8)	RF(ml_4)	RF(ml_5)	RF(nf_all)
0.2	84.737 ± 1.551	84.186 ± 1.683	82.142 ± 1.618	78.510 ± 1.538	76.485 ± 1.409	75.429 ± 1.290	88.951 ± 2.208
0.4	90.749 ± 1.738	90.185 ± 1.796	88.007 ± 1.783	83.849 ± 1.626	81.011 ± 1.574	79.460 ± 1.552	95.987 ± 1.283
0.6	93.423 ± 1.661	92.680 ± 1.595	90.843 ± 1.747	86.760 ± 1.740	83.504 ± 1.666	81.897 ± 1.641	96.907 ± 1.053
0.8	94.821 ± 1.502	93.998 ± 1.537	92.594 ± 1.689	88.705 ± 1.812	85.392 ± 1.809	83.569 ± 1.730	97.150 ± 0.981
1.0	95.590 ± 1.387	95.009 ± 1.396	93.755 ± 1.592	90.200 ± 1.807	86.947 ± 1.827	85.031 ± 1.774	97.131 ± 1.043
1.2	96.101 ± 1.310	95.585 ± 1.366	94.832 ± 1.546	92.697 ± 1.652	89.772 ± 1.873	88.176 ± 1.851	97.110 ± 1.027
2.0	96.866 ± 1.174	96.424 ± 1.192	96.055 ± 1.252	94.711 ± 1.475	92.581 ± 1.781	91.113 ± 1.852	96.676 ± 1.229
3.0	97.162 ± 1.094	96.697 ± 1.118	96.537 ± 1.200	95.793 ± 1.317	94.310 ± 1.567	93.478 ± 1.713	96.235 ± 1.312
4.0	97.184 ± 1.063	96.819 ± 1.113	96.778 ± 1.088	96.333 ± 1.246	95.201 ± 1.467	94.563 ± 1.573	95.908 ± 1.438
5.0	97.264 ± 1.065	96.858 ± 1.128	96.873 ± 1.104	96.545 ± 1.172	95.831 ± 1.306	95.226 ± 1.429	95.608 ± 1.482

Table 31: Results for the Thyroid Disease dataset.

BR	RF(nt_500)	RF(qs_ent)	RF(mn_4)	RF(mn_8)	RF(ml_4)	RF(ml_5)	RF(nf_all)
0.2	92.821 ± 2.404	92.992 ± 2.334	93.078 ± 2.393	92.924 ± 2.317	89.785 ± 2.068	82.280 ± 3.670	93.146 ± 2.386
0.4	95.148 ± 1.951	94.949 ± 1.940	95.049 ± 2.068	94.822 ± 2.099	93.696 ± 2.220	93.371 ± 2.124	93.927 ± 2.296
0.6	95.529 ± 1.952	95.478 ± 1.831	95.384 ± 2.054	95.166 ± 2.103	94.431 ± 2.199	94.229 ± 2.256	94.203 ± 2.366
0.8	95.552 ± 1.945	95.675 ± 1.848	95.366 ± 1.938	95.087 ± 2.067	94.631 ± 2.131	94.496 ± 2.179	94.142 ± 2.378
1.0	95.542 ± 1.926	95.766 ± 1.841	95.331 ± 1.981	95.070 ± 2.055	94.710 ± 2.176	94.531 ± 2.210	94.080 ± 2.362
1.2	95.624 ± 1.903	95.840 ± 1.777	95.482 ± 1.917	95.240 ± 1.968	95.010 ± 2.091	94.870 ± 2.109	94.078 ± 2.288
2.0	95.459 ± 1.935	95.635 ± 1.858	95.328 ± 1.924	95.112 ± 2.057	94.964 ± 2.034	94.815 ± 2.110	93.763 ± 2.308
3.0	95.321 ± 2.021	95.565 ± 1.853	95.152 ± 2.030	95.029 ± 2.010	94.882 ± 2.139	94.778 ± 2.179	93.689 ± 2.327
4.0	95.217 ± 2.047	95.523 ± 1.882	95.042 ± 2.059	94.924 ± 2.080	94.847 ± 2.193	94.768 ± 2.280	93.622 ± 2.378
5.0	95.163 ± 2.044	95.423 ± 1.924	94.977 ± 2.058	94.898 ± 2.041	94.858 ± 2.108	94.724 ± 2.113	93.601 ± 2.347

Table 32: Results for the Vehicle Silhouettes dataset.

BR	RF(nt_500)	RF(qs_ent)	RF(mn_4)	RF(mn_8)	RF(ml_4)	RF(ml_5)	RF(nf_all)
0.2	72.444 ± 1.686	72.441 ± 1.739	72.170 ± 1.746	71.441 ± 1.810	70.228 ± 1.823	69.615 ± 1.790	72.351 ± 1.817
0.4	73.467 ± 1.615	73.362 ± 1.587	73.238 ± 1.683	72.954 ± 1.710	71.817 ± 1.768	71.322 ± 1.774	73.385 ± 1.837
0.6	73.932 ± 1.618	73.790 ± 1.564	73.845 ± 1.625	73.434 ± 1.670	72.490 ± 1.695	71.973 ± 1.794	73.595 ± 1.680
0.8	74.286 ± 1.606	74.070 ± 1.560	74.118 ± 1.673	73.737 ± 1.597	72.794 ± 1.692	72.355 ± 1.770	73.597 ± 1.682
1.0	74.397 ± 1.591	74.227 ± 1.509	74.303 ± 1.614	73.998 ± 1.663	73.005 ± 1.694	72.568 ± 1.683	73.656 ± 1.709
1.2	74.442 ± 1.581	74.322 ± 1.568	74.347 ± 1.608	74.212 ± 1.590	73.451 ± 1.695	73.160 ± 1.646	73.471 ± 1.747
2.0	74.557 ± 1.519	74.487 ± 1.561	74.566 ± 1.615	74.422 ± 1.555	73.948 ± 1.619	73.616 ± 1.683	73.220 ± 1.765
3.0	74.506 ± 1.542	74.434 ± 1.576	74.531 ± 1.562	74.455 ± 1.597	74.127 ± 1.618	74.071 ± 1.574	72.681 ± 1.856
4.0	74.544 ± 1.480	74.547 ± 1.582	74.480 ± 1.529	74.522 ± 1.562	74.214 ± 1.536	74.138 ± 1.563	72.343 ± 1.885
5.0	74.583 ± 1.512	74.442 ± 1.576	74.544 ± 1.577	74.505 ± 1.549	74.326 ± 1.665	74.276 ± 1.495	72.091 ± 1.918

Table 33: Results for the Vowel Recognition dataset.

BR	RF(nt_500)	RF(qs_ent)	RF(mn_4)	RF(mn_8)	RF(ml_4)	RF(ml_5)	RF(nf_all)
0.2	84.796 ± 2.104	81.707 ± 2.151	80.631 ± 2.235	76.111 ± 2.369	73.027 ± 2.420	70.847 ± 2.581	77.066 ± 2.491
0.4	88.552 ± 1.902	86.939 ± 2.015	85.794 ± 2.090	82.279 ± 2.149	78.848 ± 2.342	76.617 ± 2.353	82.283 ± 2.336
0.6	90.170 ± 1.852	89.077 ± 1.852	88.036 ± 1.943	85.067 ± 2.124	81.585 ± 2.264	79.443 ± 2.321	84.474 ± 2.194
0.8	90.981 ± 1.737	90.127 ± 1.732	89.185 ± 1.881	86.562 ± 2.053	83.281 ± 2.128	81.293 ± 2.266	85.400 ± 2.053
1.0	91.415 ± 1.745	90.697 ± 1.694	89.849 ± 1.804	87.463 ± 2.015	84.339 ± 2.210	82.412 ± 2.172	85.844 ± 2.090
1.2	91.657 ± 1.692	91.089 ± 1.653	90.576 ± 1.767	89.089 ± 1.895	86.603 ± 2.078	85.111 ± 2.154	86.088 ± 2.145
2.0	92.146 ± 1.616	91.751 ± 1.686	91.428 ± 1.663	90.328 ± 1.796	88.485 ± 1.956	87.211 ± 2.098	85.754 ± 2.149
3.0	92.285 ± 1.651	91.964 ± 1.601	91.718 ± 1.651	91.034 ± 1.757	89.755 ± 1.855	88.989 ± 1.876	84.890 ± 2.276
4.0	92.278 ± 1.662	91.929 ± 1.679	91.785 ± 1.722	91.363 ± 1.701	90.404 ± 1.804	89.876 ± 1.829	84.246 ± 2.288
5.0	92.182 ± 1.667	91.922 ± 1.652	91.730 ± 1.719	91.492 ± 1.683	90.832 ± 1.729	90.358 ± 1.742	83.619 ± 2.390

Table 34: Results for the Wine dataset.

BR	RF(nt_500)	RF(qs_ent)	RF(mn_4)	RF(mn_8)	RF(ml_4)	RF(ml_5)	RF(nf_all)
0.2	97.548 ± 1.432	96.649 ± 1.856	96.674 ± 1.847	96.444 ± 1.891	96.413 ± 1.915	96.435 ± 1.965	95.716 ± 2.252
0.4	97.632 ± 1.363	97.067 ± 1.751	97.034 ± 1.743	96.840 ± 1.767	96.489 ± 1.785	96.447 ± 1.870	95.309 ± 2.617
0.6	97.694 ± 1.358	97.346 ± 1.619	97.298 ± 1.603	97.191 ± 1.642	96.677 ± 1.761	96.581 ± 1.755	95.073 ± 2.973
0.8	97.728 ± 1.347	97.368 ± 1.575	97.424 ± 1.519	97.331 ± 1.563	96.691 ± 1.697	96.579 ± 1.758	95.132 ± 3.017
1.0	97.764 ± 1.381	97.396 ± 1.578	97.455 ± 1.534	97.357 ± 1.560	96.728 ± 1.773	96.581 ± 1.807	94.927 ± 3.137
1.2	97.809 ± 1.312	97.416 ± 1.630	97.441 ± 1.528	97.385 ± 1.601	96.969 ± 1.638	96.812 ± 1.721	94.916 ± 3.081
2.0	97.761 ± 1.340	97.416 ± 1.663	97.567 ± 1.513	97.455 ± 1.559	97.039 ± 1.675	96.938 ± 1.789	94.067 ± 3.291
3.0	97.654 ± 1.465	97.362 ± 1.615	97.489 ± 1.541	97.452 ± 1.581	97.211 ± 1.682	97.051 ± 1.713	93.492 ± 3.291
4.0	97.649 ± 1.445	97.357 ± 1.639	97.500 ± 1.509	97.511 ± 1.513	97.334 ± 1.598	97.272 ± 1.595	93.101 ± 3.373
5.0	97.640 ± 1.421	97.329 ± 1.648	97.492 ± 1.536	97.438 ± 1.560	97.289 ± 1.612	97.236 ± 1.604	92.812 ± 3.454

Table 35: Results for the Ringnorm dataset.

BR	RF(nt_500)	RF(qs_ent)	RF(mn_4)	RF(mn_8)	RF(ml_4)	RF(ml_5)	RF(nf_all)
0.2	89.752 ± 2.383	88.622 ± 2.779	89.057 ± 2.718	90.107 ± 2.605	83.540 ± 3.072	81.078 ± 3.104	81.605 ± 3.569
0.4	92.597 ± 2.220	91.437 ± 2.413	91.802 ± 2.314	92.443 ± 2.212	89.123 ± 2.691	87.778 ± 2.827	86.065 ± 3.641
0.6	92.717 ± 2.390	91.538 ± 2.526	91.962 ± 2.455	92.335 ± 2.352	89.738 ± 2.701	88.995 ± 2.848	86.747 ± 3.468
0.8	92.370 ± 2.473	91.515 ± 2.582	92.060 ± 2.533	92.192 ± 2.413	89.898 ± 2.675	89.288 ± 2.742	86.725 ± 3.669
1.0	92.173 ± 2.457	91.325 ± 2.692	91.710 ± 2.543	91.957 ± 2.376	89.828 ± 2.619	89.232 ± 2.687	86.767 ± 3.679
1.2	91.977 ± 2.513	91.010 ± 2.693	91.407 ± 2.617	91.657 ± 2.539	90.160 ± 2.638	89.562 ± 2.832	86.563 ± 3.737
2.0	91.322 ± 2.523	90.442 ± 2.754	91.068 ± 2.593	91.213 ± 2.590	89.865 ± 2.754	89.453 ± 2.837	85.672 ± 3.747
3.0	90.670 ± 2.640	89.985 ± 2.752	90.365 ± 2.661	90.450 ± 2.597	89.757 ± 2.755	89.432 ± 2.788	84.672 ± 4.002
4.0	90.398 ± 2.648	89.603 ± 2.710	90.092 ± 2.730	90.173 ± 2.691	89.680 ± 2.698	89.405 ± 2.692	84.085 ± 3.918
5.0	90.173 ± 2.731	89.312 ± 2.864	89.882 ± 2.666	89.953 ± 2.717	89.555 ± 2.733	89.473 ± 2.724	83.438 ± 3.954

Table 36: Results for the Threenorm dataset.

BR	RF(nt_500)	RF(qs_ent)	RF(mn_4)	RF(mn_8)	RF(ml_4)	RF(ml_5)	RF(nf_all)
0.2	79.700 ± 2.653	77.880 ± 2.842	77.762 ± 2.973	77.563 ± 2.958	77.197 ± 2.973	76.840 ± 2.982	76.652 ± 3.294
0.4	80.050 ± 2.774	78.720 ± 2.921	78.812 ± 3.059	78.557 ± 2.957	78.468 ± 3.065	78.128 ± 3.138	77.513 ± 3.275
0.6	79.888 ± 2.623	79.040 ± 2.823	79.040 ± 2.753	78.963 ± 2.746	78.587 ± 2.734	78.342 ± 2.820	77.258 ± 3.135
0.8	79.852 ± 2.690	78.910 ± 2.977	79.252 ± 2.782	79.035 ± 2.856	78.733 ± 2.997	78.667 ± 2.891	77.218 ± 3.254
1.0	79.743 ± 2.617	78.723 ± 2.892	78.977 ± 2.792	79.025 ± 2.736	78.643 ± 2.856	78.505 ± 2.890	77.008 ± 3.304
1.2	79.725 ± 2.693	78.715 ± 2.903	78.967 ± 2.861	78.958 ± 2.820	78.868 ± 2.887	78.702 ± 2.938	76.598 ± 3.262
2.0	79.465 ± 2.681	78.663 ± 2.941	78.810 ± 2.659	78.925 ± 2.822	78.687 ± 2.827	78.528 ± 2.833	75.537 ± 3.555
3.0	79.032 ± 2.749	78.307 ± 2.811	78.503 ± 2.890	78.525 ± 2.860	78.390 ± 2.811	78.465 ± 2.860	74.313 ± 3.647
4.0	78.843 ± 2.693	78.053 ± 2.910	78.422 ± 2.954	78.313 ± 2.865	78.407 ± 2.845	78.373 ± 2.859	73.457 ± 3.735
5.0	78.810 ± 2.787	77.863 ± 3.004	78.178 ± 2.904	78.312 ± 2.964	78.258 ± 2.877	78.285 ± 2.944	72.995 ± 3.860

Table 37: Results for the Twonorm dataset.

BR	RF(nt_500)	RF(qs_ent)	RF(mn_4)	RF(mn_8)	RF(ml_4)	RF(ml_5)	RF(nf_all)
0.2	96.002 ± 1.397	94.825 ± 1.692	95.023 ± 1.634	94.927 ± 1.780	94.755 ± 1.720	94.590 ± 1.751	93.297 ± 2.170
0.4	95.688 ± 1.426	94.630 ± 1.742	94.977 ± 1.651	94.730 ± 1.676	94.363 ± 1.747	94.192 ± 1.831	92.850 ± 2.546
0.6	95.413 ± 1.533	94.360 ± 1.774	94.805 ± 1.646	94.540 ± 1.722	94.070 ± 1.728	93.942 ± 1.788	91.957 ± 2.703
0.8	95.285 ± 1.560	94.297 ± 1.800	94.567 ± 1.745	94.467 ± 1.717	93.993 ± 1.833	93.722 ± 1.836	91.260 ± 2.948
1.0	95.093 ± 1.594	93.975 ± 1.833	94.448 ± 1.804	94.253 ± 1.723	93.770 ± 1.740	93.625 ± 1.911	90.832 ± 3.036
1.2	95.008 ± 1.634	93.957 ± 1.825	94.355 ± 1.727	94.288 ± 1.867	93.797 ± 1.901	93.678 ± 1.893	90.383 ± 3.141
2.0	94.617 ± 1.728	93.653 ± 2.006	94.123 ± 1.838	94.038 ± 1.772	93.542 ± 2.007	93.307 ± 1.991	88.787 ± 3.731
3.0	94.413 ± 1.814	93.378 ± 1.957	93.923 ± 1.828	93.955 ± 1.892	93.438 ± 1.949	93.322 ± 2.010	87.398 ± 3.882
4.0	94.197 ± 1.846	93.200 ± 1.975	93.628 ± 1.848	93.807 ± 1.884	93.425 ± 1.977	93.302 ± 2.006	86.270 ± 4.283
5.0	94.125 ± 1.866	93.057 ± 1.966	93.680 ± 1.917	93.647 ± 1.897	93.435 ± 1.907	93.342 ± 1.969	85.280 ± 4.206

Table 38: Results for the Waveform dataset.

BR	RF(nt_500)	RF(qs_ent)	RF(mn_4)	RF(mn_8)	RF(ml_4)	RF(ml_5)	RF(nf_all)
0.2	86.165 ± 2.424	84.730 ± 2.706	84.752 ± 2.666	84.630 ± 2.705	84.067 ± 2.777	83.598 ± 2.739	83.990 ± 2.788
0.4	85.635 ± 2.441	84.913 ± 2.489	84.702 ± 2.578	84.658 ± 2.591	84.900 ± 2.591	84.465 ± 2.553	82.855 ± 3.023
0.6	85.328 ± 2.322	84.747 ± 2.563	84.375 ± 2.433	84.313 ± 2.561	84.857 ± 2.639	84.725 ± 2.619	81.982 ± 3.297
0.8	84.868 ± 2.409	84.538 ± 2.441	84.253 ± 2.667	84.253 ± 2.515	84.823 ± 2.576	84.827 ± 2.616	81.252 ± 3.185
1.0	84.682 ± 2.396	84.367 ± 2.447	83.973 ± 2.479	83.970 ± 2.690	84.660 ± 2.573	84.632 ± 2.539	80.578 ± 3.406
1.2	84.435 ± 2.406	84.135 ± 2.592	83.998 ± 2.537	83.910 ± 2.563	84.552 ± 2.562	84.598 ± 2.650	80.015 ± 3.251
2.0	83.948 ± 2.494	83.758 ± 2.533	83.332 ± 2.500	83.327 ± 2.731	84.000 ± 2.582	84.058 ± 2.684	78.445 ± 3.620
3.0	83.585 ± 2.478	83.368 ± 2.600	83.293 ± 2.563	83.230 ± 2.704	83.788 ± 2.702	83.740 ± 2.625	77.073 ± 3.826
4.0	83.485 ± 2.539	83.398 ± 2.528	83.177 ± 2.706	83.073 ± 2.593	83.507 ± 2.534	83.590 ± 2.503	76.318 ± 3.853
5.0	83.437 ± 2.509	83.282 ± 2.544	83.083 ± 2.552	83.055 ± 2.503	83.230 ± 2.609	83.468 ± 2.596	75.653 ± 3.977

Table 39: Results for the LED Display Domain dataset.

BR	RF(nt_500)	RF(qs_ent)	RF(mn_4)	RF(mn_8)	RF(ml_4)	RF(ml_5)	RF(nf_all)
0.2	61.648 ± 3.594	57.242 ± 4.151	58.780 ± 4.167	61.237 ± 3.791	57.737 ± 4.245	54.337 ± 4.506	63.862 ± 3.841
0.4	63.392 ± 3.392	61.350 ± 3.712	62.823 ± 3.885	65.780 ± 3.654	64.990 ± 3.818	64.850 ± 3.512	64.633 ± 3.597
0.6	63.365 ± 3.434	61.950 ± 3.708	62.835 ± 3.763	65.375 ± 3.708	65.847 ± 3.627	66.018 ± 3.704	62.800 ± 3.736
0.8	63.285 ± 3.478	61.343 ± 3.613	62.977 ± 3.735	64.765 ± 3.697	65.703 ± 3.673	66.425 ± 3.750	61.330 ± 3.704
1.0	63.025 ± 3.481	61.593 ± 3.608	63.047 ± 3.787	64.528 ± 3.715	65.448 ± 3.790	66.590 ± 3.755	60.175 ± 3.837
1.2	62.818 ± 3.516	61.617 ± 3.801	62.740 ± 3.485	64.327 ± 3.701	64.993 ± 3.476	65.320 ± 3.472	59.453 ± 3.951
2.0	62.553 ± 3.622	61.428 ± 3.795	62.062 ± 3.696	63.653 ± 3.511	64.565 ± 3.620	65.050 ± 3.650	57.205 ± 4.111
3.0	62.110 ± 3.544	60.918 ± 3.705	61.262 ± 3.575	62.790 ± 3.642	63.873 ± 3.489	64.218 ± 3.450	55.770 ± 4.185
4.0	61.888 ± 3.528	61.000 ± 3.822	61.155 ± 3.752	62.073 ± 3.700	63.287 ± 3.582	63.932 ± 3.513	55.203 ± 4.229
5.0	61.848 ± 3.570	61.240 ± 3.724	60.912 ± 3.687	61.622 ± 3.713	62.742 ± 3.714	63.420 ± 3.666	54.860 ± 4.338

C Bootstrap Rate Curves

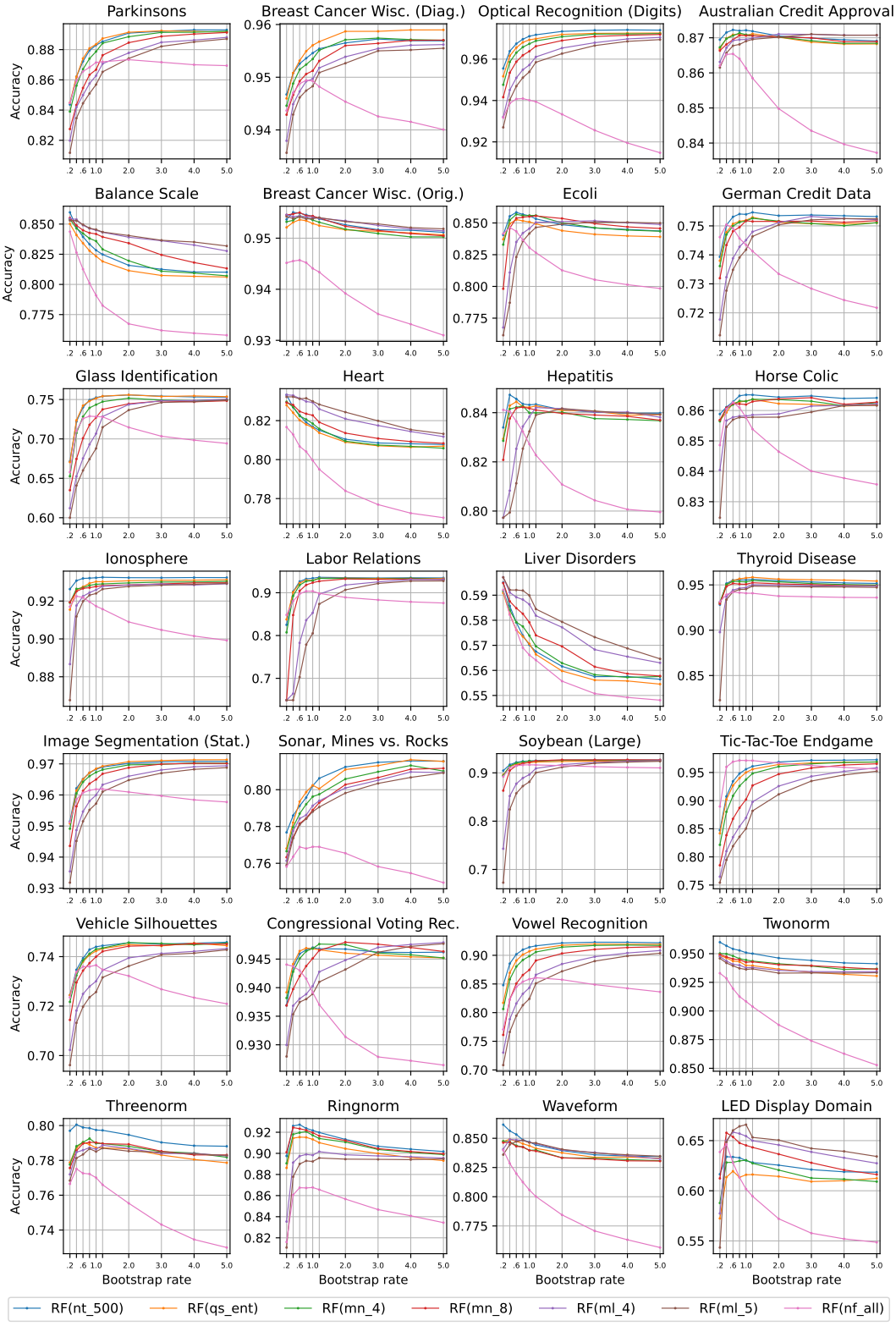

Figure 4: Characteristics of bootstrap rate curves for datasets not shown in Fig. 2.